



UNIVERSITÀ DEGLI STUDI DI PALERMO

Dottorato di Ricerca in Biomedicina e Neuroscienze  
Dipartimento di Biomedicina, Neuroscienze e Diagnostica avanzata  
SSD BIO/16

UNIVERSITÀ DEGLI STUDI DI PALERMO

## **Neuropathological Alterations after Smoke Inhalation Injury, with and without Skin Burn**

LA CANDIDATA  
**Dott.ssa Anita Randolph**

II COORDINATORE  
**Prof. Fabio Bucchieri**

IL CO-TUTOR  
**Chiar.mo Prof. Maria- Adelaide Micci**

LA TUTOR  
**Prof. Francesco Cappello**

---



UNIVERSITÀ DEGLI STUDI DI PALERMO

CICLO XXXII  
ANNO CONSEGUIMENTO TITOLO 2018/2019



UNIVERSITÀ DEGLI STUDI DI PALERMO

---



UNIVERSITÀ DEGLI STUDI DI PALERMO

**Neuropathological Alterations after Smoke Inhalation Injury,  
with and without Skin Burn**

UNIVERSITÀ DEGLI STUDI DI PALERMO

by

**Anita Randolph, BS, BSA**

**Dissertation**

Presented for the requirements

toward the completion

for the Degree of

**Doctorate of Philosophy**

**The University of Palermo**

**November, 2019**

---



UNIVERSITÀ DEGLI STUDI DI PALERMO



UNIVERSITÀ **Dedication** DI PALERMO

I would like to dedicate this work to my grandparents, Vinson and Anne Randolph for encouraging me unconditionally personally and academically.





---

## Acknowledgements

First, I would like to thank Dr. Micci for serving as the guarantor for my project. I am greatly appreciative for the opportunity to work in her laboratory. In the short time, I was a member; she helped me to improve my scientific and professional skills. I gained tremendously from the support of the members of Dr. Micci's laboratory: Elizabeth Bishop, Austin Cody Grant, Jutatip Guptarak, and Emanuele Mocchiario.

Secondly, I would like to thank all of my graduation committee members Dr. Tagliatela, Dr. Porter, Dr. Hamill, and Dr. Olsen for their support and dedication in grooming my project. I would like to especially thank Dr. Hamill for always making time to critique my experimental design and for challenging me to improve my writing and scientific skills.

Thirdly, I would also like to thank all the members (Ayotola Akinola, Randi Bolding, Haley Flowers, Kang Ko, Christina Nelson, Cynthia Moncebiaz, Randy Salsbury, Ryan Scott, and Ashley Smith) of the Translational Intensive Care Unit for technical assistance with the sheep surgeries, post-surgery monitoring and collection of hemodynamic data.

---

Lastly, I would like to thank the Research Histopathology Core manager Kenneth Escobar for histopathology training. This project would not have been possible without his commitment to training me to complete all of my studies.



---

## **Neuropathological Alterations after Smoke Inhalation Injury, with and without Skin Burn**

More than 23,000 smoke inhalation injuries are reported in the United States each year. While the pathophysiology of smoke inhalation-induced lung injury is well studied, little is known about the acute effects of smoke inhalation on the central nervous system (CNS). Tragic events, such as those of the nightclub fire in Brazil in 2013, suggest that neurological complications occur following smoke inhalation injury, with the most commonly reported symptoms being a persistent headache, memory loss, and paresthesia. Additionally, one case report described that smoke inhalation alone was associated with progressive cognitive and psychiatric impairments, lasting for years after the initial injury, with neurological dysfunctions starting within one-month post-injury and persisting for over 14 years. These reports lead to the conclusion that acute smoke inhalation injury results in a long-term global decrease in metabolic activity and deterioration of several areas of the brain. In this study, using a well-characterized ovine model, we aimed to characterize acute pathophysiological changes in the brain induced by smoke inhalation, with and without third-degree skin burn injury. Our data show that smoke inhalation, regardless of the presence of third-degree skin burn, leads to diffuse histopathological changes in the brain and loss of blood-brain barrier integrity resulting in dilated and congested blood vessels and micro-hemorrhaging. These findings provide important information that can be used to develop effective and novel treatment options for patients with smoke and burn injuries aimed at alleviating CNS dysfunction.

---

## TABLE OF CONTENTS

List of Figures .....	x
List of Abbreviations.....	xii
Chapter 1 Introduction .....	13
Smoke Inhalation Injury.....	13
Pathophysiology of Smoke Inhalation Injury .....	13
Burn Injury.....	16
Pathophysiology of Burn Injury.....	16
CNS Dysfunction following Smoke Inhalation Injury.....	17
The Nervous System .....	18
Sheep and Human Neuroanatomy: Similarities and Differences.....	19
Brain Regions of Interest .....	20
Chapter 2 Materials & Methods .....	23
Why the Sheep model of Smoke Inhalation ± Third-degree Skin Burn .....	23
Animal Compliance and Use .....	24
Surgical Catheterization of Sheep in Preparation for Injury .....	24
Smoke Inhalation ±Third-degree Skin Burn .....	25
Post-injury Care .....	26
Fluid Resuscitation.....	27
Tissue Collection.....	27
Tissue Processing.....	28
Histological Staining.....	29
Luxol Fast Blue counterstained with Hematoxylin & Eosin .....	29
Periodic acid-Schiff Stain .....	30
Maritus Scarlet Blue Stain .....	31
Albumin Immunohistochemistry .....	32
Quantification.....	32
Statistical Analysis.....	33

---

Chapter 3 Results .....	33
The Sheep Model of Smoke Inhalation Injury ± Third-degree Skin Burn Results in Damage to the CNS. ....	33
Hypoxia levels and Hemodynamics are not Different between Smoke Inhalation Injury ± Third-degree Skin Burn. ....	36
Smoke Inhalation Injury ± Third-degree Skin Burn Results in an Increase of Dilated and Congested Blood Vessels throughout the Brain.....	38
Smoke Inhalation Injury ± Third-degree Skin Burn Caused a Significant Decrease in Normal Blood Vessels.....	41
Smoke Inhalation Injury ± Third-degree Skin Burn Caused a Significant Decrease in the Number of Normal Blood Vessels. ....	43
Smoke Inhalation Injury ± Third-degree Skin Burn Resulted in the Increase of the Percent Total Dilated Vessels vs. Total Blood Vessels throughout the Brain.....	45
The Integrity of Blood Vessels Basement Membrane is Lost following Smoke Inhalation Injury ± Third-degree Skin Burn. ....	47
Smoke Inhalation Injury ± Third-degree Skin Burn Resulted in Dilated Blood Vessels that Ruptured in the Brain.....	51
Smoke Inhalation Injury ± Third-degree Skin Burn Resulted in an Increase in the Percent of Ruptured Blood Vessels in the Brain.....	54
Smoke Inhalation Injury Caused an Increase in Dilated Vessels that Ruptured in the Brain.....	55
Smoke Inhalation Injury ± Third-degree Skin Burn Resulted in Microhemorrhaging in the Brain.....	57
Confirmation of Microhemorrhaging following Smoke Inhalation Injury ± Third-degree Skin Burn by Positive MSB Staining.....	60
Smoke Inhalation Injury ± Third-degree Skin Burn Resulted in BBB Dysfunction in the Brain confirmed by Positive Albumin Staining. ....	63
Smoke Inhalation Injury ± Third-degree Skin Burn Resulted in Neutrophil Infiltration in the Brain. ....	66
Chapter 4 Discussion.....	68
Smoke Inhalation Injury ± Third-degree Skin Burn Causes Bleeding in the Lateral Ventricles and Macrohemorrhaging throughout the Brain.....	69
Smoke Inhalation Injury ± Third-degree Skin Burn Causes BBB Dysfunction Characterized by Congested and Dilated Blood Vessels throughout the Brain.....	71
Smoke Inhalation Injury ± Third-degree Skin Burn Causes BBB Dysfunction Characterized by Congested and Dilated Blood Vessels That Rupture throughout the Brain. ....	72

---

Smoke Inhalation Injury ± Third-degree Skin Burn Resulted in Microhemorrhaging throughout the Brain.....	74
Confirmation of Microhemorrhaging following Smoke Inhalation Injury ± Third-degree Skin Burn by Positive MSB Staining throughout the Brain. .....	74
Smoke Inhalation Injury ± Third-degree Skin Burn Resulted in Neutrophil Infiltration throughout the Brain.....	75
Chapter 5 Conclusion.....	76
Bibliography.....	77
Vita	85

## List of Figures

Figure 1:	Smoke inhalation ± third-degree skin burn caused bleeding in the lateral ventricles and hemorrhaging throughout the brain. ....	35
Figure 2:	Blood brain barrier dysfunction following smoke inhalation ± third-degree skin burn is not a result of hypoxia during injury or changes in hemodynamics during the first 48-hour post-injury.....	37
Figure 3:	Luxol fast blue/ H&E staining revealed smoke inhalation ± third-degree skin burn caused BBB dysfunction characterized by congested and dilated blood vessels throughout the brain.....	41
Figure 4A:	Smoke inhalation ± third-degree skin burn caused a significant decrease in normal blood vessels throughout the brain. ....	43
Figure 4B:	Smoke inhalation ± third-degree skin burn caused a significant decrease in the total percent of normal blood vessels throughout the brain. ....	45
Figure 4C:	Smoke inhalation ± third-degree skin burn resulted in an increase of dilated blood vessels versus total vessels throughout the brain. ....	47
Figure 5:	Confirmation of BBB dysfunction following smoke inhalation ± third-degree skin burn by positive PAS staining. ....	50
Figure 6:	Luxol fast blue/ H&E staining revealed smoke inhalation ± third-degree skin burn caused BBB dysfunction characterized by congested and dilated blood vessels that ruptured throughout the brain. ....	53

Figure 7A:	Smoke inhalation ± third-degree skin burn caused an increase in the percent total ruptured versus total blood vessels throughout the brain.	55
Figure 7B:	Smoke inhalation ± third-degree skin burn caused an increase in the congested and dilated blood vessels in the brain that ruptured.	57
Figure 8:	Luxol fast blue/ H&E staining reveals smoke inhalation ± third-degree skin burn resulted in microhemorrhaging throughout the brain.	59
Figure 9:	Confirmation of microhemorrhaging following smoke inhalation ± third-degree skin burn by positive MSB staining throughout the brain.	63
Figure 10:	Smoke inhalation ± third-degree skin burn resulted in microhemorrhaging in the brain confirmed by positive albumin staining.	65
Figure 11:	Smoke inhalation ± third-degree skin burn resulted in neutrophil infiltration into the brain.	68



## List of Abbreviations

ABA	American Burn Association
BBB	blood brain barrier
CNS	central nervous system
CVP	central venous pressure
Co-Hb	carboxyhemoglobin
H&E	hematoxylin and eosin
IHC	immunohistochemistry
IL	interleukin
IM	intramuscular
IV	intravenous
LAP	left atrium pressure
LFB	Luxol fast blue
MAP	mean arterial pressure
MPAP	mean pulmonary artery pressure
MSB	Martius, Scarlet, and Blue stain
NO	nitric oxide
NVU	neurovascular unit
PAS	Periodic acid–Schiff stain
PET	positron emission tomography
PNS	peripheral nervous system
ROS	reactive oxygen species
RNS	reactive nitrogen species
SR	slow release
sub-Q	subcutaneously
TBSA	total body surface area
TICU	Translational Intensive Care Unit
WHO	World Health Organization

## **Chapter 1 Introduction**

### **SMOKE INHALATION INJURY**

Each year, more than 23,000 smoke inhalation injuries are reported in the United States (1). The shift from the use of natural to synthetic materials and petrochemicals has dramatically increased the complexity of toxic gases inhaled after ignition, thereby increasing the likelihood of inhalation injury after combustion (2). Tragic events such as the terrorist attacks on the World Trade Center and the Pentagon in 2001 and the nightclub fire in Brazil in 2013 were associated with high incidents of smoke-inhalation injury (3, 4). Specifically, inhalation of toxic compounds present in the dust and smoke during the World Trade Center attack was reported to cause 49% of inhalation injuries of the 790 survivors in the first 48-hours (3, 4). Additionally, according to the World Health Organization (WHO), inhalation of smoke generated from indoor cooking, forest fires, and burning crops leads to more than 1 billion cases of airway and pulmonary inflammation each year (5).

### **PATHOPHYSIOLOGY OF SMOKE INHALATION INJURY**

The pathophysiology of smoke inhalation injury is well-characterized and studied in humans (6). The first 48-hours following injury is characterized by a hypermetabolic response that results in an increased circulation of proinflammatory cytokines and catecholamines (6-8). Pathophysiologic changes include decreased cardiac output and

blood flow to organs, airway obstruction, reduced gas exchange, and a hyperactive airway (2, 6-8). During the chronic phase, there is an increase in oxygen consumption, pulmonary edema, protein wasting, and an altered mental status due to heavy sedation (2, 6-8).

Inhalation injury is divided into three categories based on area of damage: 1) thermal injury mostly affecting the upper airway due to thermal injury to the mouth, oropharynx, and larynx; 2) chemical and particulate irritation to the lower airway and parenchymal tissue of the lungs; and 3) metabolic asphyxiation from toxic gases such as CO and cyanide (2, 9, 10). The upper airway is the primary site of injury resulting from inhalation of high temperatures. Damage is localized above the vocal cords affecting the oro- and nasopharynx due to rapid heat exchange (2, 11). Burns of the nasal and oropharyngeal mucosa, edema, erythema, ulceration, and epithelial damage appear in the first 22-36 hours post-injury (2, 12). The tracheobronchial system area is injured affecting vasomotor and sensory nerve ending.

Particulate matter deposition is a consequence of inhaling compounds such as soot, aldehydes, nitrogen oxides, and hydrochloric acid further exacerbating injury (2, 12). Deposition of particulates also results in decreased compliance and an increase in mechanical obstruction and airway resistance from cast (protein-rich profuse transudate) formation (2, 12). Systemic toxicity occurs as a result of inflammation and production of oxygen free radicals (2, 12).

The molecular cascade of inhalation injury begins with the direct thermal injury to the upper airway damaging the epithelial layer and denaturing proteins. This leads to the activation of the complement cascade and subsequent release of histamine and xanthine

oxidase (2). Histamine further stimulates damaged endothelial cells to secrete high levels of nitric oxide (NO) (2). Xanthine oxidase breakdown proteins and release superoxide, a reactive oxygen species (ROS), and purines (2). Reactive nitrogen species (RNS) such as peroxynitrite are also increased due to NO and ROS reacting (2, 13). In combination, both ROS and RNS result in airway edema (2). Cytokines such as interleukin- 8 (IL-8) lead to the recruitment of monocytes further stimulating the inflammatory response (2, 14). Additionally, smoke inhalation stimulates the sensory nerve endings and vasomotor in the tracheobronchial area to release neuropeptides inducing neurogenic inflammation (2). Under physiological conditions, neuropeptidases neutralize toxic agents by secreting neutral endopeptidases (2). However, due to the cellular injury of epithelial cells, this neutralizing capability is lost (2, 15). Instead, neuropeptidases attract and activate neutrophils resulting in further release of ROS. ROS and RNS can also interact with DNA or lipids via oxidation, nitration or nitrosylation, and proteins resulting in single-stranded breaks in the DNA (2, 16). The DNA repair enzyme poly(ADP ribose) polymerase (PARP) are activated not only by breaks in the DNA but also by NO and RNS production (2, 17, 18). The activation of PARP further exacerbate inflammation by depleting the cell of adenosine triphosphate (ATP) leading to cellular dysfunction and apoptosis in addition to activation of nuclear factor  $\kappa$ B (NF-  $\kappa$ B) (2). Attraction and activation of polymorphonuclear (PMN) cells, upregulation of IL-8, iNOS (inducible nitric oxide synthase) formation, and NO production result from the activation of NF-  $\kappa$ B. An increase in RNS results from the reaction of NO and ROS thereby creating a positive feedback loop leading to more DNA damage and PARP activation (2, 19). Proinflammatory mediators are then circulated systemically from the lung, bronchial and

pulmonary vasculature, to systemic organs (2).

## **BURN INJURY**

The American Burn Association (ABA) reports that in 2015 there were 203,422 burn injuries that required some degree of medical attention in the United States (20). While thermal burns account for 42.6% of all burn injuries, injuries caused by fire and flame account for the majority of medically treated burns (20). Between 2% and 30% of burn patients with thermal injuries from fires suffer from combined burn and smoke inhalation injury that greatly increases their morbidity and mortality (12).

## **PATHOPHYSIOLOGY OF BURN INJURY**

The skin is the largest organ of the body, performing many functions such as protection against external damage, thermoregulation, sensory, and neuroendocrine (21). There are three layers that form the skin: 1) epidermis 2) dermis 3) and the hypodermis or subcutaneous tissue (21-23). Burn injuries are classified by evaluating the depth of injury to the skin. The extent of damage is dependent on the time of exposure and duration, the percentage of TBSA, and the source of the injury (22, 24-26). Loss of the dermis and damage to the subcutaneous tissue layer is characteristic of a third-degree burn. These feel leathery to the touch, charred, dry, and require ventilator support (24).

Large burns, > 30% TBSA, are associated with severe tissue destruction (27, 28). Systemic effects result from the release of numerous inflammatory mediators such as cytokines, catecholamines, and antidiuretic hormones from the site of injury and distant

sites as well (27-32). There are two distinct phases of the systemic effect following injury, burn shock and hypermetabolic phase (27-29, 33, 34). The burn shock phase occurs within the first 24-48 hours after a major burn. Pathophysiological changes include generalized edema extending from injured to noninjured areas (27-29, 34). Plasma leakage into the area of injury and extensive edema into noninjured areas over 48 hours can result in burn shock (27, 29, 34). Clinically, loss of intravascular fluid into burned areas coupled with edema manifests as impaired tissue and organ perfusion (27, 29, 34). As a result of decreased intravascular volume, heart rate and increased pulmonary and systemic vascular resistance cardiac output is decreased (29, 33-35). Additional clinical complications that occur in burn shock are decreased urine output, compartment syndrome, and poor oxygenation (27-29). The hypermetabolic phase begins 48-hours after injury defined by increased blood flow to vital organs, carbon dioxide production, and cardiac output (27, 29, 34).

#### **CNS DYSFUNCTION FOLLOWING SMOKE INHALATION INJURY**

There is limited information available regarding the effects of smoke inhalation ± third-degree skin burn on the central nervous system (CNS). Despite the fact that advances in clinical care and the development of novel treatments have greatly increased the survival of burn-injury and smoke inhalation injury patients, as of today, very few follow up studies on pathological alterations of the CNS and associated cognitive dysfunctions have been conducted.

Neurological complications such as a persistent headache, memory loss, and paresthesia (abnormal sensation such as tingling with no physical stimulation) were

reported in survivors of the nightclub fire in Brazil in 2013 that suffered smoke inhalation injuries (3). In one clinical report, a progressive decline in neurological functions was reported after a single acute combustible smoke inhalation incident (36). Specifically, complications started within one-month post-injury and included headache, anhedonia (inability to feel pleasure from normally pleasurable activities), impaired concentration, and reduced attention and learning skills (36). Cognitive impairments such as difficulty in word finding, bradyphrenia (slowness of thought), and reduced short and long-term memory were also reported (36). Additionally, positron emission tomography (PET) showed decreased metabolic activity in the entire brain three years post-injury (36), and follow-up PET scan, 14 years post-injury, revealed areas of continued deterioration (corpus callosum, orbital frontal lobes, globus pallidus, putamen, and thalamus). Most importantly, although there were areas of increased glucose metabolism, none of the areas returned to normal control values over the time of observation (36). These studies suggest that neurological and cognitive impairments occur as a result of smoke inhalation and prompts the need of more extensive characterizations of CNS pathological changes following smoke inhalation ± third-degree skin burn.

## **THE NERVOUS SYSTEM**

The nervous system can be divided into two categories: the central nervous system (CNS) and the peripheral nervous system (PNS). The PNS is comprised of millions of spinal and cranial nerves fibers responsible for transmitting sensory information to and from the CNS (37). These nerves innervate the entire body including

the skin, muscles, organs, and glands controlling somatic and autonomic, voluntary and involuntary processes of the body (37).

#### **SHEEP AND HUMAN NEUROANATOMY: SIMILARITIES AND DIFFERENCES**

There are several similarities and differences between the neuroanatomy of the sheep and human. In both the sheep and human, the brain and spinal cord make up the CNS and is encapsulated by the skull and vertebral columns (37). The surface of the cerebral cortex is characterized by folds and ridges, gyri, flanked by furrows, sulci, resulting in increased cortical surface area of the brain of the sheep and human (37). The sulcus and gyrus are one major characteristic that separates sheep neuroanatomy from common rodent models used in research such as rats, mice, and guinea pigs. A distinguishable difference between the sheep and human brain is size. The average human brain weighs about three pounds or about 2% of their body weight (37). The brain of the sheep is far much less, weighing around 0.40 pounds or about 0.3% of their body weight.

The sheep and human brain can be subdivided into the cerebrum (two cerebral hemispheres and diencephalon), cerebellum, and brainstem (37). The cerebrum is the largest structure of the CNS composed of two cerebral hemispheres, separated by the longitudinal fissure into the left and right hemisphere, and the diencephalon (37). The hippocampus and basal ganglia are the major subcortical areas of the cerebrum. Each cerebral hemisphere is divided into five lobes: frontal lobe, parietal lobe, occipital lobe, temporal lobe, and limbic lobe (37). The frontal lobe begins at the most anterior tip of the brain extending to the lateral sulcus separating it from the parietal lobe and temporal lobe



on the lateral surface (37). The frontal lobe has four general functional areas: primary motor cortex (initiation of voluntary movements), premotor and supplementary motor areas (initiation of voluntary movements), Broca's area (production of written and spoken language), and the prefrontal cortex (executive functions such as personality, insight, and foresight) (37). Extending from the central sulcus to the preoccipital sulcus is the parietal lobe (37). The three functions of the parietal lobe are primary somatosensory cortex (processing tactile and proprioceptive information), inferior parietal lobule together with the temporal lobe (comprehension of language), and spatial orientation and directing attention (37). The temporal lobe extends superiorly from the lateral sulcus towards the preoccipital sulcus (37). The temporal lobe is responsible for primary auditory cortex, Wernicke's area (comprehension of language), higher-order processing of visual information, and learning and memory (37). The occipital lobe extends from the lateral sulcus and parietoccipital sulcus (37). The major function of the occipital lobe is visual functions since it is comprised of the primary visual cortex and the visual association cortex (higher-order processing of visual information) (37). The limbic lobe is observed from the medial surface of the brain where it wraps around the telencephalon and diencephalon (37). The limbic lobe houses the hippocampus and the amygdala and is tasked with emotional response, drive-related behavior, and memory (37).

### **BRAIN REGIONS OF INTEREST**

The frontal cortex spans the entire anterior cerebral cortex of the frontal lobes. The subdivisions of the frontal cortex are organized into three regions: the orbital, lateral, and medial regions (38). Additionally, there are several Brodmann areas housed in the

frontal cortex that are essential in complex movement, executive cognition, behavior, reasoning, emotion, and speech (38).

The basal ganglia are thought of as the area of the brain responsible for movement disorders (37, 39). The basal ganglia are comprised of a group of deeply embedded subcortical nuclei responsible for motor learning, executive functions and behaviors, and emotions (37, 39). There are five major nuclei that comprise the basal ganglia: the striatum (caudate nucleus, nucleus accumbens, and putamen), globus pallidus (external and internal segment), subthalamic nucleus, substantia nigra (compact part and reticular part), and the lenticular nucleus (37, 39). These nuclei form multiple parallel loops important in sending, receiving, and relaying information from several regions of the brain.

The limbic lobe houses the hippocampus and the amygdala and is tasked with the emotional response, drive-related behavior, and memory (37). The amygdala is located beneath the uncus of the temporal lobe anterior to the hippocampus, where it extends continuously anteriorly from the tail of the caudate nucleus and posteriorly from the putamen (37). The nuclei that comprise the amygdala are subdivided into three categories: medial, central, and basolateral groups. Each of the nuclei is involved in different functions. The medial nuclei of the amygdala are interconnected to the olfactory system where it receives smell information directly from the olfactory bulb or the olfactory cortex (37). The central nuclei receive afferent visceral sensory information from the hypothalamus and the brainstem (periaqueductal gray and parabrachial nuclei) (37). The emotional response is mediated by the basolateral nuclei, interconnecting the

hypothalamus and specific nuclei of the brainstem (37). Efferent fibers of the amygdala mainly project to the cerebral cortex and the hypothalamus (37).

The second major structure of the limbic system is the hippocampus, located in the temporal lobe (37). The main function of the hippocampus is consolidation of information from short-term memory into long-term memory, more specifically declarative memory (remembering facts and events) (37). Declarative memory is subdivided into episodic and semantic memory. This is made possible by afferent projections from the entorhinal cortex passes information from the association cortex such as the posterior cingulate gyrus, orbital cortex, and multimodal areas of the frontal cortex, parietal, and temporal lobes (37). The major efferent pathways of the hippocampus extend to the fornix projecting to the thalamus, hypothalamus, and the mammillary body (37).

The cerebellum has several functions including motor skill acquisition, processing somatosensory, vestibular visual information, auditory and cognitive functions (37). The afferent pathways to the cerebellum arrive from several areas of the brain including the locus cereleus, the raphe nucleus, and cerebral cortex (pontine nuclei) (37). At the cerebellar cortex, afferent fibers, mossy and climbing fibers, end on Purkinje cells and dendrites of granular cells. Purkinje cells project to the deep nuclei, which acts as the primary efferent pathway from the cerebellum (37).

The brainstem connects the brain to the spinal cord and can be divided into four prominent structures: the medulla oblongata, pons, and midbrain (37, 40). The pons is located inferior to the midbrain and superior to the medulla oblongata, and anteriorly to the cerebellum. The pons received the name due to the appearance of a protruding mass

resembling a bridge, which interconnects the two cerebellar hemispheres and the cerebellum. The characteristic shape of the pons is a result of abundant pontine nuclei that form the pontocerebellar pathway (37, 40). Functions of the pons include control of consciousness, breathing, heart rate, and blood pressure (37, 40).

The pituitary gland is located at the base of the brain deep in the skull enclosed in a protective bony cavity, the sella turcica (41). The anterior, intermediate, and posterior lobes together form the pituitary gland. The anterior lobe is the largest of the three lobes by size and weight and produces several hormones that regulate reproduction, growth, and stress (41). Collectively, the lobes of the pituitary gland are responsible for secreting several hormones such as thyroid stimulating hormone, growth hormone, follicle stimulating hormone, adrenocorticotropic hormone, luteinizing hormones, and anti-diuretic hormone (41).

In this study, I used an established ovine model to characterize pathological changes in the CNS observed following smoke inhalation  $\pm$  third-degree skin burn injury, with a focus on blood-brain barrier damages and related structural changes throughout the brain. I hypothesize that smoke inhalation, regardless of the presence of third-degree skin burn, leads to blood-brain barrier dysfunction.

## **Chapter 2 Materials & Methods**

### **WHY THE SHEEP MODEL OF SMOKE INHALATION $\pm$ THIRD-DEGREE SKIN BURN**

Over the past 50 years our laboratory, Translational Intensive Care Unit (TICU), has proven the ovine model of severe lung injury following inhalation with or without

third-degree skin burn, has several advantages over a mouse model. The first advantage of using ovine is the similarity of the pulmonary anatomy to humans, especially the bronchial circulation. This anatomy is not present in rodents and the lack of bronchial submucosal glands, therefore excluding them as good models for this injury. Secondly, the genomics and the host responses of ovine to various diseases/pathology are similar to humans, which is unlike in the rodents. Thirdly, precise ventilator control, continuous hemodynamic monitoring and fluid resuscitation are required following acute cardiopulmonary injury as a result of smoke inhalation. Due to the large mass of the ovine, which can be better monitored in a large animal such a sheep.

#### **ANIMAL COMPLIANCE AND USE**

This study was completed in compliance with the National Institutes of Health Office of Animal Welfare and approved by the Institutional Animal Care and Use Committee of the University of Texas Medical Branch.

#### **SURGICAL CATHETERIZATION OF SHEEP IN PREPARATION FOR INJURY**

Twenty-three female Merino sheep between 30 – 40 kg were surgically prepped with multiple vascular catheters for hemodynamic monitoring during the experimental period (42). In preparation for surgery, female sheep were deeply anesthetized using ketamine (KetaVed, Phoenix Scientific, St. Joseph, MO), both intramuscular (IM) and intravenous (IV), followed by 5% isoflurane (IsoSol, VEDCO, St. Joseph, MO) via an endotracheal tube. To avoid discomfort, a long-acting analgesia (0.005- 0.01 mg/kg of

buprenorphine slow release (SR)) (Buprenorphine SR<sup>TM</sup>, SR Veterinary Technologies, Windsor, CO) was administered subcutaneously (sub-Q) immediately before starting the operation. During surgery, sheep were surgically instrumented with 1) vascular catheters in the common pulmonary artery via the right jugular vein, 2) the abdominal aorta via the right femoral artery, and 3) the left atrium via the left thoracotomy at the level of the fifth intercostal space to conduct hemodynamic monitoring. After the surgery, sheep were allowed to recover five to seven days with free access to food and water. Buprenorphine was given when needed for postsurgical analgesia.

#### **SMOKE INHALATION ±THIRD-DEGREE SKIN BURN**

After the surgical recovery, catheterized sheep were exposed to smoke inhalation ± third-degree skin burn. Before the injury, baseline values of hemodynamics were obtained by connecting catheters to pressure transducers (model PX4X4, Baxter Edwards Critical Care Division, Irvine, CA) in the healthy state. Prior to injury, sheep were randomly assigned to one of three groups: 1) sham group, n=8 (surgery, but no injury), 2) smoke only, n=8 (48 breaths of cooled cotton smoke), and 3) combined smoke inhalation and third-degree skin burn, n=7 (48 breaths of cooled cotton smoke and third-degree skin burn over 40% TBSA). Prior to inducing inhalation injury and third-degree skin burn, all sheep underwent tracheostomy (10mm diameter, Shiley, Irvine, CA), by published procedures (43). All injuries were performed under deep anesthesia (2-5% isoflurane) and analgesia (0.005- 0.01 mg/kg of buprenorphine SR). The smoke used for injury was prepared by burning 40g of cotton towels (42). Smoke inhalation was induced by insufflation of 48 breaths of cooled cotton smoke via a tracheostomy tube using a

modified bee smoker. Arterial blood gas samples were collected and analyzed using a blood gas analyzer (RAPIDPoint 500 System, Siemens Healthcare Diagnostics, Tarrytown, NY) to determine carboxyhemoglobin (Co-Hb) levels, immediately after every four sets of twelve breaths of smoke insufflation. To ensure comparable injury between all injury groups, the temperature of the smoke was not allowed to exceed 40°C (42). The temperature is not allowed to exceed 40°C to 1) replicate lung injury due to the chemicals in the smoke and not thermal injury, and 2) mimic the heat exchange that naturally occurs by the oro- and nasopharynx (42). The temperature of the smoke was measured by inserting a Swan- Ganz catheter (model 131F7, Edwards Critical Care Division, Irvine, CA) into a modified endotracheal tube, connected to the modified bee smoker. Sheep in the smoke inhalation and combined injury groups received the same 48 breathes of cooled cotton smoke inhalation as described above, and were additionally subjected to third-degree skin burn over 40% of the TBSA via Bunsen burner (44).

#### **POST-INJURY CARE**

Following injury, sheep were transferred to the TICU, and immediately placed on mechanical ventilation (Hamilton-G5, Hamilton Medical, Switzerland) support using APVcmv mode with positive end-expiratory pressure set at 5 cm H<sub>2</sub>O and monitored for 48 hours in a conscious state. Tidal volume was maintained at 12mL/kg and a respiratory rate of 20 breaths per minute. To accelerate dissociation of carbon monoxide from hemoglobin, sheep received 100% oxygen for the first three hours following injury. Additionally, arterial oxygen tension was maintained above 95 mmHg by adjusting the fraction of inspiratory oxygen. Hemodynamics measurements (mean arterial pressure

(MAP); central venous pressure (CVP); mean pulmonary artery pressure (MPAP); and left atrium pressure (LAP) were recorded on a monitor with graphics and digital displays (MP30, Philips, Andover, MA). Pulmonary function, blood for the preparation of serum, and blood gas exchange were recorded every six hours in the conscious state. All hemodynamics were recorded while sheep were calm and at a standing position. To ensure recording was taken at the same position every six hours, hemodynamics were recorded after the transducer was placed at the olecranon joint on the frontal leg while the sheep were standing.

#### **FLUID RESUSCITATION**

To compensate for the severe fluid loss in both injury groups, fluid resuscitation using lactated Ringer's solution were calculated using the Parkland formula. To ensure accurate measurement of fluid intake during the 48-hour monitoring post-injury, sheep were allowed free access to food but not water.

#### **TISSUE COLLECTION**

48-hours after smoke inhalation  $\pm$  third-degree skin burn, sheep were euthanized by IV administration of xylazine (0.2mg/kg), ketamine (10-15mg/kg), and buprenorphine (0.005-0.01mg/kg). Sheep brains were collected and divided in half by a sagittal cut down the longitudinal fissure; one-half was fixed in 10% buffered formalin, and the other one-half was snap-frozen in liquid nitrogen and stored at  $-80^{\circ}\text{C}$ . After three weeks, formalin fixed brains were sliced in several coronal sections, 0.5 inches in thickness, with



the first cut through the mammillary bodies. Brain areas of interest were collected based on data demonstrating the frontal cortex, basal ganglia, amygdala, hippocampus, thalamus, cerebellum, pons, and pituitary gland showing the most damage. Additionally, blood was collected for preparing serum for analysis every 6 hours after induction of injury.

UNIVERSITÀ DEGLI STUDI DI PALERMO

### **TISSUE PROCESSING**

The frontal cortex, basal ganglia, amygdala, hippocampus, cerebellum, pons, and pituitary gland were collected and placed into a cassette (Thermo Shandon™, Thermo Fisher Scientific, Waltham, MA) for processing (Pathcentre, Thermo Shandon™, Thermo Fisher Scientific, Waltham, MA). The brain areas of interest were processed for embedding through several rounds of fixative, alcohol, xylene, and paraffin. In brief, tissue sections were stirred with agitation in 10% buffered formalin (StatLab, McKinney, TX) at ambient temperature under vacuum and pressure for two hours. This was followed by several rounds of 70%, 80%, 95% alcohol (StatLab, McKinney, TX) with agitation at ambient temperature under vacuum and pressure for four hours each round. The tissue sections were subjected to three rounds of 100% alcohol (StatLab, McKinney, TX) at ambient temperature under vacuum and pressure for two hours for the first two rounds and one hour for the last round. Next, three rounds of xylene (StatLab, McKinney, TX) at ambient temperature under vacuum and pressure for two hours for the first two rounds and one hour for the last round. Lastly, the tissue samples were subjected to four rounds of paraffin (Parapro XLT, StatLab, McKinney, TX) at 60°C under vacuum and pressure for one hour for the first three rounds and two hours for the last round. After processing,

tissue were paraffin embedded (Embedding Console System, Tanner Scientific™, Sarasota, FL) and sectioned (Microm HM 3255, Thermo Scientific, Waltham, MA) 4-5 μm thick.

## **HISTOLOGICAL STAINING**

In preparation for staining, all slices were deparaffinized and hydrated with three rounds of xylene, 100% alcohol, and two rounds 95% alcohol for five minutes each round.

### **LUXOL FAST BLUE COUNTERSTAINED WITH HEMATOXYLIN & EOSIN**

To assess BBB dysfunction, any structural changes to blood vessel integrity, sections were stained with Luxol Fast Blue (LFB) and counterstained with H&E. LFB/solvent blue 38 (Sigma Chemical, St. Louis, MO) was preheated to 80°C in a water bath (Precision™, ThermoFisher Scientific, Waltham, MA). After deparaffinization, slides were incubated in LFB for 30 minutes. After the incubation period, slices were allowed to cool at room temperature for 30 minutes. Slides were rinsed in 95% alcohol with agitation, then placed in fresh 95% alcohol for five minutes. To clear the remaining LFB, slides were rinsed in running tap water for five minutes. Slides were differentiated by dipping in 0.05% Lithium carbonate (J.T. Baker Chemical Co. Phillipsburg, NJ) and 70% alcohol until the gray matter was void of staining leaving the white matter blue. The slides were counterstained with H&E (Varistain® Gemini automatic stainer, Thermo Scientific). A) Frontal cortex; sham n= 8, smoke inhalation injury n= 7, smoke + third-

degree skin burn n = 7, B) Basal ganglia; sham n=8, smoke inhalation injury n=7, smoke + third-degree skin burn n =6, C) Amygdala; sham n=8, smoke inhalation injury n=5, smoke + third-degree skin burn n =7, D) Hippocampus; sham n=7, smoke inhalation injury n=7, smoke + third-degree skin burn n =6, E) Pons, F) Cerebellum, Grey matter; G) Cerebellum, granule layer; sham n=8, smoke inhalation injury n=5, smoke + third-degree skin burn n =7, and H) and pituitary gland; sham n=6, smoke inhalation injury n=5, smoke + third-degree skin burn n =5.

#### **PERIODIC ACID-SCHIFF STAIN**

The integrity of the basement membranes of blood vessels was evaluated by staining with Periodic acid–Schiff (PAS). Preceding staining, 5 µm coronal sections were deparaffinized and rehydrated. The slides were incubated in 0.5% periodic acid (Fisher Scientific, Fair Lawn, NJ) for five minutes at room temperature and rinsed in deionized water. The slides were then treated with Schiff Reagent solution (Fischer Scientific, Fair Lawn, NJ) for ten minutes followed by washing in tap water for an additional ten minutes. Following staining, slides were counterstained with Mayer’s hematoxylin (Polyscientific R&D Corp, Bay Shore, NY) for five minutes and rinsed clean with 0.15% acid alcohol (dH<sub>2</sub>O, 100% alcohol, 6mL HCl). A) Frontal cortex; sham n=8, smoke inhalation injury n=8, smoke + third-degree skin burn n=7, B) Basal ganglia; sham n=8, smoke inhalation injury n=8, smoke + third-degree skin burn n =7, C) Amygdala; sham n=7, smoke inhalation injury n=7, smoke + third-degree skin burn n =7, D) Hippocampus; sham n=7, smoke inhalation injury n=7, smoke + third-degree skin burn n =7, E) Pons; sham n=6, smoke inhalation injury n=6, smoke + third-degree skin burn n

=6, F) Cerebellum, Grey matter, G) Cerebellum, granule layer; sham n=7, smoke inhalation injury n=6, smoke + third-degree skin burn n =7 H) and pituitary gland; sham n=6, smoke inhalation injury n=5, smoke + third-degree skin burn n =5.

#### **MARITUS SCARLET BLUE STAIN**

4-5  $\mu$ m thick coronal sections were stained with MSB for histopathology confirmation of hemorrhaging following smoke inhalation injury  $\pm$  third-degree skin burn. To stain the nuclear chromatin, deparaffinized slides were incubated in Weigert's Hematoxylin (Polyscientific R&D Corp, Bay Shore, NY) for fifteen minutes and rinsed clean in running tap water for five minutes. The slides were treated with 1% acid alcohol for ten seconds and washed clean in running tap water for five minutes. The slides were rinsed in 95% alcohol with agitation and stained in Martius (Pfaltz & Bauer, Waterbury, CT) for two minutes at room temperature. The slides were rinsed in running tap water and stained in brilliant crystal 6R for ten minutes and rinsed again in running tap water. The slides were incubated with 1% phosphotungstic acid (Fischer Scientific, Fair Lawn, NJ) for ten minutes and rinsed in running tap water. This was followed by staining with 0.5% aniline blue (Fisher Scientific, Fair Lawn, NJ) for ten minutes, then rinsed in running tap water. A) Frontal cortex; sham n=7, smoke inhalation injury n=8, smoke + third-degree skin burn n =7 B) Basal ganglia; sham n=7, smoke inhalation injury n=8, smoke + third-degree skin burn n =7, C) Amygdala; sham n=7, smoke inhalation injury n=6, smoke + third-degree skin burn n =7, D) Hippocampus; sham n=6, smoke inhalation injury n=8, smoke + third-degree skin burn n =6, E) Pons; sham n=6, smoke inhalation injury n=7, smoke + third-degree skin burn n =6 F) Cerebellum, Grey matter, G)

Cerebellum granule layer; sham n=7, smoke inhalation injury n=7, smoke + third-degree skin burn n =6, and H) pituitary gland; sham n=7, smoke inhalation injury n=5, smoke + third-degree skin burn n =6.

### **ALBUMIN IMMUNOHISTOCHEMISTRY**

To confirm neurovascular dysfunction of the BBB, 4-5  $\mu\text{m}$  thick coronal sections were stained with mouse anti-albumin antibody (1:50; Abcam Cambridge, MA). Following deparaffinization, slides underwent antigen retrieval by incubating in Tris/EDTA pH 9 (Sigma Chemical, St. Louis, MO) at 95°C for twenty minutes before staining. A) Frontal cortex; sham n=6, smoke inhalation injury n=5, smoke + third-degree skin burn n =7, B) Basal ganglia; sham n=8, smoke inhalation injury n=7, smoke + third-degree skin burn n=7, C) Amygdala; sham n=8, smoke inhalation injury n=7, smoke + third-degree skin burn n=7, D) Hippocampus; sham n=8, smoke inhalation injury n=6, smoke + third-degree skin burn n =6, E) Pons; sham n=6, smoke inhalation injury n=7, smoke + third-degree skin burn n =7, F) Cerebellum, sham n=8, smoke inhalation injury n=5 , smoke + third-degree skin burn n =7, and G) pituitary gland; sham n=6, smoke inhalation injury n=5, smoke + third-degree skin burn n =7.

### **QUANTIFICATION**

The total area of positive staining of the PAS and MSB sections were quantified using the Keyence BZ-X700 all-in-one fluorescence microscope (Itasca, IL). The counts of microhemorrhaging, neutrophils, normal, dilated, and ruptured blood vessels were

completed by using ImageJ (NIH). All quantification was performed on at least five 10x magnification images taken at random throughout the field of view.

#### **STATISTICAL ANALYSIS**

GraphPad Prism 7 (La Jolla, CA) was used to perform statistical analysis. Data are expressed as the mean $\pm$  standard error of the mean (SEM). Differences between groups were determined by one-way ANOVA and Tukey's multiple comparison tests. Differences were considered significant for  $P < 0.05$ .

### **Chapter 3 Results**

In this study, I used an established ovine model to characterize pathological changes in the CNS following smoke inhalation  $\pm$  third-degree skin burn injury, with a focus on blood-brain barrier damages and related structural changes throughout the brain. I hypothesize that smoke inhalation, regardless of the presence of third-degree skin burn, leads to blood-brain barrier dysfunction.

#### **THE SHEEP MODEL OF SMOKE INHALATION INJURY $\pm$ THIRD-DEGREE SKIN BURN RESULTS IN DAMAGE TO THE CNS.**

The experimental sheep model of smoke inhalation  $\pm$  third-degree skin burn was induced by insufflation of cooled cotton smoke and third-degree skin burn over 40% TBSA (44). Gross examination of three-week postmortem 0.5 inches thick coronal brain

sections of sheep subjected to smoke inhalation ± third-degree skin burn injury revealed severe bleeding throughout the brain. The lateral ventricles were enlarged and blood clots were present due to intraventricular hemorrhage (**Figure 1B**). In several coronal sections, enlargement of the lateral ventricles resulted in a shift in the midline (**Figure 1B**). In rare cases, rupture of the lateral ventricles resulted in bleeding in the brain parenchyma. Hemorrhagic infarcts and micro-bleeds were observed diffusely throughout the brain (**Figure 1B**). From this, areas of interest were identified as being most affected by smoke inhalation ± third-degree skin burn. These areas of interest are the frontal cortex, basal ganglia, amygdala, hippocampus, pons, thalamus, cerebellum, and the pituitary (**Figure 1C**).

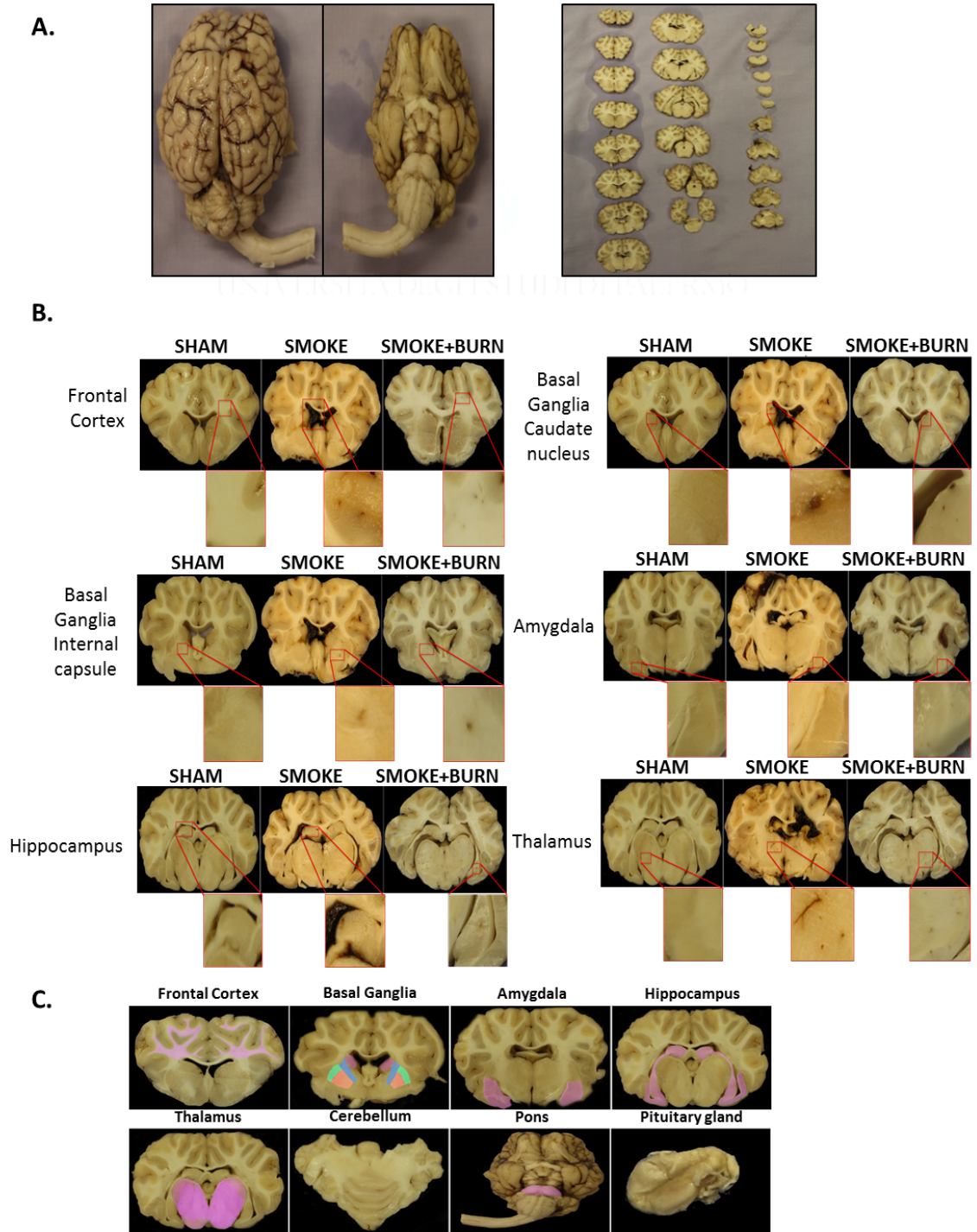


Figure 1: Smoke inhalation ± third-degree skin burn caused bleeding in the lateral ventricles and hemorrhaging throughout the brain.



A) Anterior and posterior view of sheep brain following injury. Brains were fixed in 10% buffered formalin for 3 weeks. B) Coronal sections of a three-week postmortem sheep brain post injury revealed bleeding in the lateral ventricles and macrohemorrhaging following smoke inhalation  $\pm$  third-degree skin burn. C) Coronal sections revealed the frontal cortex, basal ganglia, amygdala, hippocampus, thalamus, cerebellum, pons, and pituitary gland were damaged following injury.

**HYPOXIA LEVELS AND HEMODYNAMICS ARE NOT DIFFERENT BETWEEN SMOKE INHALATION INJURY  $\pm$  THIRD-DEGREE SKIN BURN.**

After each round of four twelve breathes of smoke insufflation, arterial carboxyhemoglobin (Co-Hb) was measured. There was no significant difference in arterial Co-Hb levels immediately after the injury between the smoke only and smoke inhalation + third-degree skin burn groups, indicating a comparable injury between the two injury groups (**Figure 2**). Analysis of the partial pressure oxygen in the arterial blood (PaO<sub>2</sub>) during inhalation injury revealed no differences in hypoxia between the groups (**Figure 2**). Thus suggesting that hypoxia is not the underlying cause of the gross CNS pathology observed following injury.

Sheep were monitored during the first 48-hours after injury in a conscious state in order to eliminate the possible effects of hemodynamic changes and hypoxia itself on the CNS pathology following injury. There were no significant changes in hemodynamics during the 48-hour experimental period in cardiac output, heart rate, mean arterial pressure, and temperature (**Figure 2**).

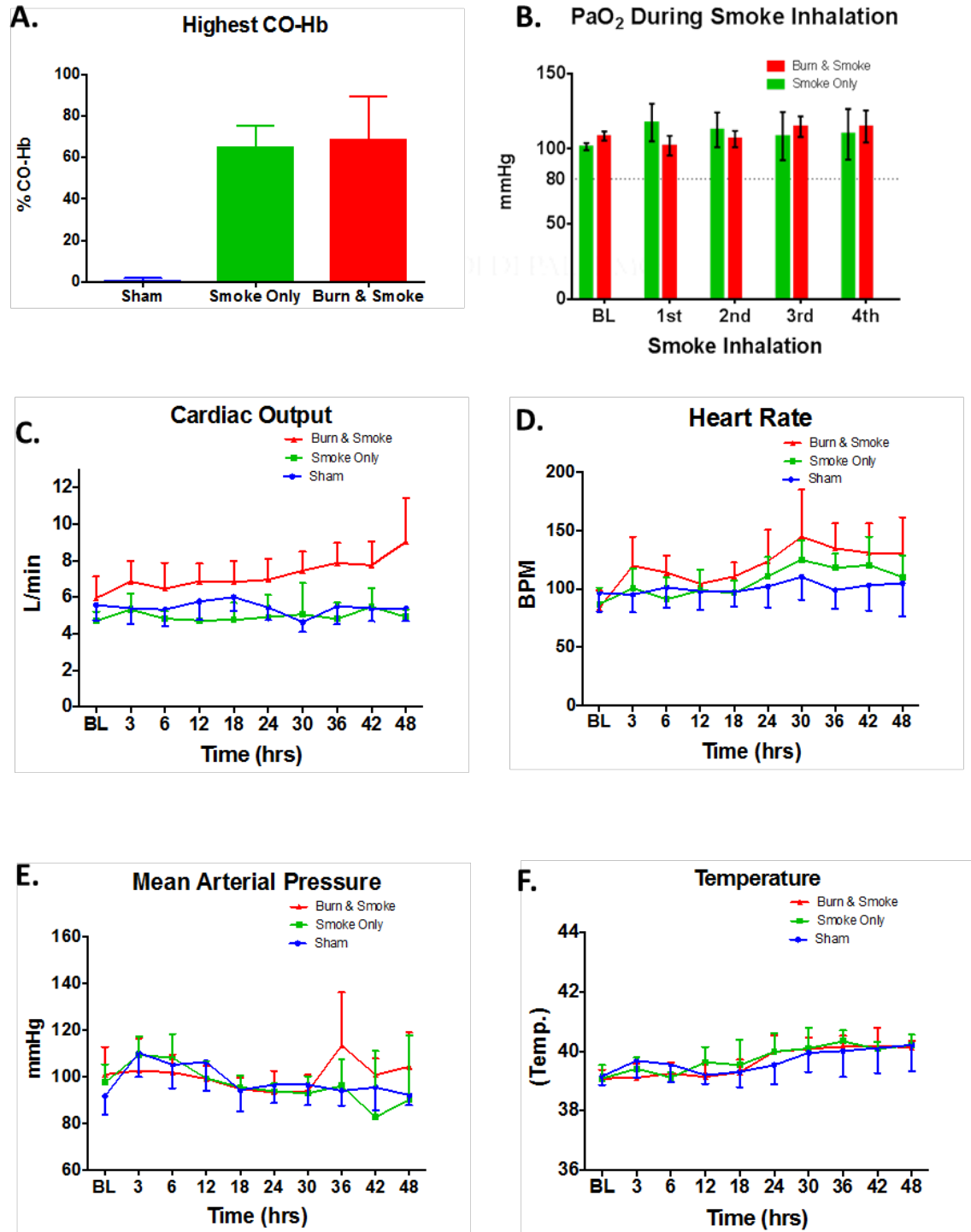


Figure 2: Blood brain barrier dysfunction following smoke inhalation ± third-degree skin burn is not a result of hypoxia during injury or changes in hemodynamics during the first 48-hour post-injury.

A) Co-Hb was not significantly different between the injury groups ( $P > 0.05$  smoke inhalation injury vs. smoke + third-degree skin burn), indicating that the injury was comparable between the groups. B)  $\text{PaO}_2$  during smoke insufflation demonstrated the sheep were not hypoxic during the smoke inhalation injury. Hemodynamics changes during the 48-hour experimental period C) cardiac output, D) heart rate, E) mean arterial pressure, and F) temperature were not different between the experimental groups, thus were not contributing factors to the pathological changes in the brain shown in Figure 1. Grouping are as followed: 1) sham group,  $n=8$  (surgery, but no injury), 2) smoke only,  $n=8$  (48 breaths of cooled cotton smoke), and 3) combined smoke inhalation and third-degree skin burn,  $n=7$  (48 breaths of cooled cotton smoke and third-degree skin burn over 40% TBSA).

#### **SMOKE INHALATION INJURY $\pm$ THIRD-DEGREE SKIN BURN RESULTS IN AN INCREASE OF DILATED AND CONGESTED BLOOD VESSELS THROUGHOUT THE BRAIN.**

Gross anatomical analysis of brains from sheep subjected to smoke inhalation  $\pm$  third-degree skin burn injury revealed numerous neuropathological changes, i.e., bleeding in the lateral ventricles and microhemorrhaging (**Figure 1**). In order to better characterize blood vessel dysfunction, 4-5 $\mu\text{m}$  sections of the frontal cortex, basal ganglia, amygdala, hippocampus, pons, cerebellum, and pituitary were stained with Luxol Fast Blue and Hematoxylin & Eosin (LFB/HE). Numerous dilated and congested blood vessels were visible in all areas examined (**Figure 3**). Quantification analyses showed that there was a significant increase in the number of dilated blood vessels following smoke inhalation  $\pm$  third-degree skin burn injury as compared to sham in all brain areas examined (**Figure 3**). Specifically, in the frontal cortex (**Figure 3**), there was a significant increase in dilated

and congested vessels between sham and the injury groups ( $p < 0.01$ , sham vs. smoke inhalation injury and  $p < 0.0001$ , sham vs. smoke + third-degree skin burn injury). There was also a significant increase in dilated vessels between the smoke inhalation group and the combined smoke + third-degree burn ( $p < 0.0001$ ). The blood vessels in the basal ganglia (**Figure 3**) also showed an increase in dilated and congested blood vessels following injury ( $p < 0.0001$ , sham vs. smoke inhalation injury and  $p < 0.0001$ , sham vs. smoke + third-degree skin burn injury) when compared to sham. There was a significant increase in the number of these augmented vessels between both injury groups ( $p < 0.05$ , smoke inhalation injury vs. smoke + third-degree skin burn injury), with the combined injury having the highest increase. Following smoke inhalation injury and the combined smoke + third-degree skin burn, we observed dilated and congested blood vessels in the amygdala (**Figure 3**) ( $p < 0.01$ , sham vs. smoke inhalation injury and  $p < 0.0001$ , sham vs. smoke + third-degree skin burn injury). There was an increase in these distorted vessels between the two injury groups, with the combined smoke + third-degree showing the highest dilated and congested blood vessels ( $p < 0.05$ , smoke inhalation injury vs. smoke + third-degree skin burn injury). In the hippocampus the increase in dilated and congested vessels was observed between sham and the injury groups ( $p < 0.01$ , sham vs. smoke inhalation injury and  $p < 0.001$ , sham vs. smoke + third-degree skin burn injury) (**Figure 3**). The cerebellum (**Figure 3**) revealed a significant increase in dilated and congested vessels between the sham and both injury groups ( $p < 0.001$ , sham vs. smoke inhalation injury and  $p < 0.0001$ , sham vs. smoke + third-degree skin burn injury). There was a significant increase in the dilated and congested vessels between the smoke inhalation

injury group and the combined smoke + third-degree injury group ( $p < 0.05$ ), with the combined injury group being the highest.

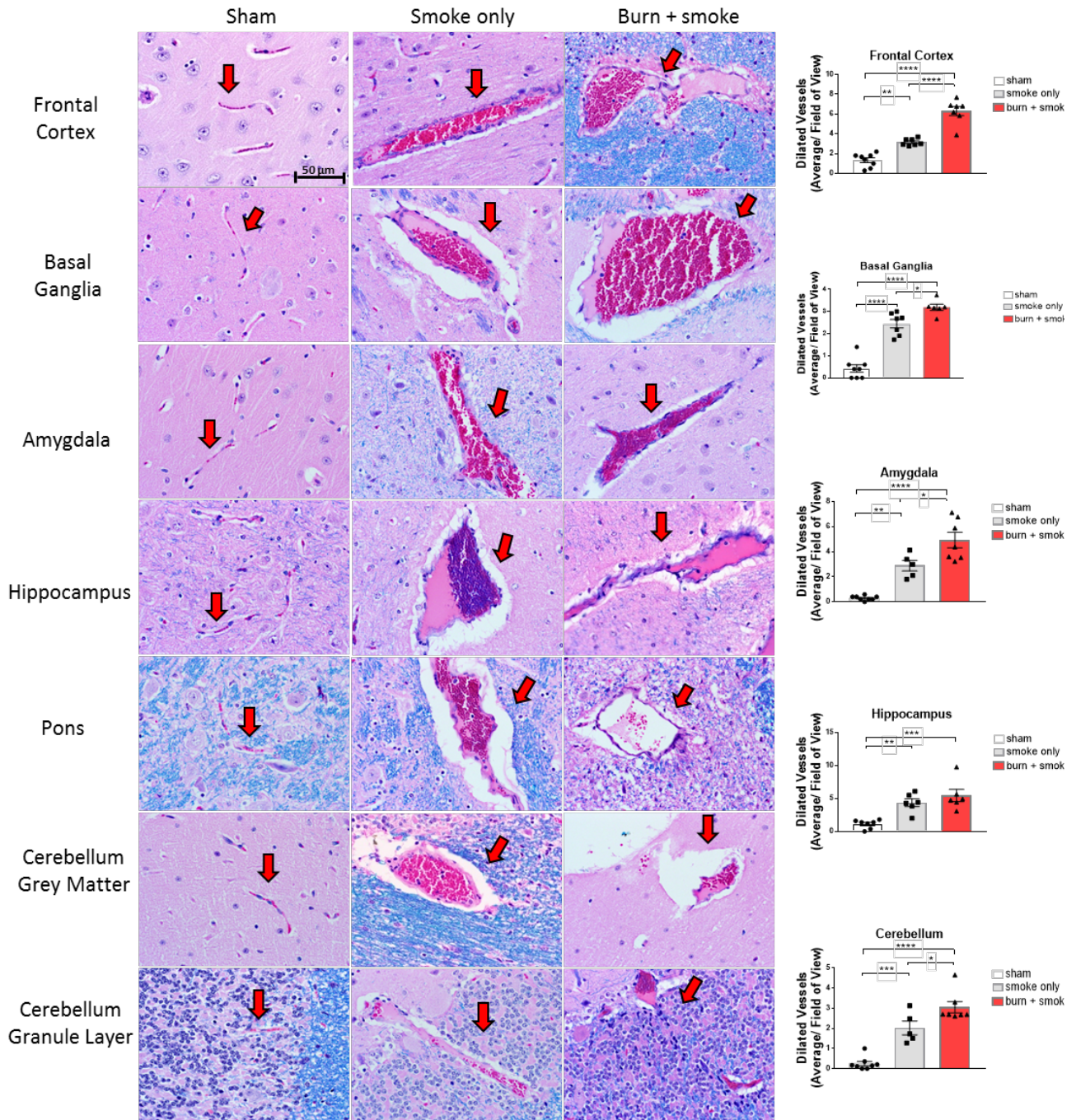


Figure 3: Luxol fast blue/ H&E staining revealed smoke inhalation ± third-degree skin burn caused BBB dysfunction characterized by congested and dilated blood vessels throughout the brain.

Representative images of sheep brain coronal sections stained with luxol fast blue (LFB) and counterstained with H&E (calibration bar = 50 mm). The graphs show the results of the quantification analyses. Following injuries, the vessels became congested and dilated in the frontal cortex, basal ganglia, amygdala, hippocampus, pons, cerebellum grey matter, and cerebellum granule layer. The red arrows denote the augmented vessels. Data are shown as mean ± SEM of 10 representative areas of each brain region of interest using one-way ANOVA with Tukey's multiple comparison test; \* p<0.05, \*\* p<0.01, \*\*\* p<0.001, \*\*\*\* p<0.0001. ). A) Frontal cortex; sham n= 8, smoke inhalation injury n= 7, smoke + third-degree skin burn n = 7, B) Basal ganglia; sham n=8, smoke inhalation injury n=7, smoke + third-degree skin burn n =6, C) Amygdala; sham n=8, smoke inhalation injury n=5, smoke + third-degree skin burn n =7, D) Hippocampus; sham n=7, smoke inhalation injury n=7, smoke + third-degree skin burn n =6, E) Pons, F) Cerebellum, Grey matter; G) Cerebellum, granule layer; sham n=8, smoke inhalation injury n=5, smoke + third-degree skin burn n =7, and H) and pituitary gland; sham n=6, smoke inhalation injury n=5, smoke + third-degree skin burn n =5.

**SMOKE INHALATION INJURY ± THIRD-DEGREE SKIN BURN CAUSED A SIGNIFICANT DECREASE IN NORMAL BLOOD VESSELS.**

We quantified the number of normal blood vessels in coronal brain sections stained with LFB/H&E and found a significant decrease in the smoke inhalation and



smoke + third-degree skin burn injury groups as compared to sham in all areas examined (**Figure 4A**). Notably, we also found a significant decrease of normal blood vessels between the smoke injury group and the combined smoke + third-degree skin burn injury group, with the combined group showing the smallest number of normal blood vessels. Specifically, in the frontal cortex the normal blood vessels were highest in the sham group with a significant decrease in the smoke inhalation injury group ( $p < 0.001$ , sham vs. smoke inhalation injury) and the combined smoke + third-degree injured group ( $p < 0.0001$ , sham vs. smoke + third-degree skin burn injury). There was also a significant decrease in normal blood vessels between the smoke inhalation injury group and the combined smoke + third-degree burn ( $p < 0.001$ , smoke inhalation injury vs. smoke + third-degree skin burn injury). The normal blood vessels in the basal ganglia showed a decrease as compared to sham in both injury groups ( $p < 0.0001$  for sham vs. both injury groups). There was also a significant decrease in the number of normal blood vessels between smoke inhalation injury and smoke + third-degree skin burn ( $p < 0.0001$ , smoke inhalation injury vs. smoke + third-degree skin burn injury). The amygdala followed the same trend as the basal ganglia with a significant decrease in normal blood vessels in the injured groups ( $p < 0.01$ , sham vs. smoke inhalation injury and  $p < 0.0001$ , sham vs. smoke + third-degree skin burn injury). There was also a decrease in normal blood vessels between the two injury groups ( $p < 0.01$ , smoke inhalation injury vs. smoke + third-degree skin burn injury). The presence of normal blood vessels in the hippocampus was significantly decreased following injury ( $p < 0.0001$ , for sham vs. both injury groups). There was a significant reduction in the number of normal blood vessels between both injury groups ( $p < 0.001$ , smoke inhalation injury vs. smoke + third-degree skin burn

injury) with the combined injury group having the least number of normal vessels. This reduction of normal blood vessels between sham and injured continued in the cerebellum ( $p < 0.0001$ , for sham vs. both injury groups). The combined injured group also revealed a significant loss of normal blood vessels when compared to smoke inhalation injury ( $p < 0.0001$ , smoke inhalation injury vs. smoke + third-degree skin burn injury).

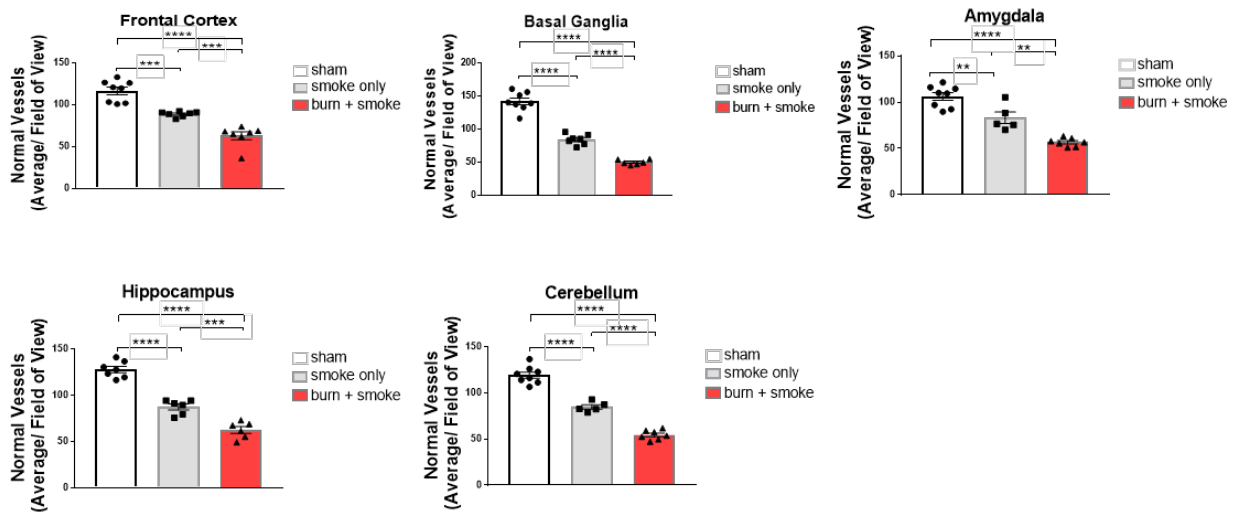


Figure 4A: Smoke inhalation ± third-degree skin burn caused a significant decrease in normal blood vessels throughout the brain.

Data are shown as mean ± SEM of 10 representative areas of each brain region of interest. One-way ANOVA with Tukey's multiple comparison tests; \*  $p < 0.05$ , \*\*  $p < 0.01$ , \*\*\*  $p < 0.001$ , \*\*\*\*  $p < 0.0001$ .

**SMOKE INHALATION INJURY ± THIRD-DEGREE SKIN BURN CAUSED A SIGNIFICANT DECREASE IN THE NUMBER OF NORMAL BLOOD VESSELS.**

We also analyzed the percent normal blood vessels in each region (Figure 4B). The frontal cortex demonstrated a decrease following smoke inhalation injury and the



combined smoke + third-degree skin burn ( $p < 0.05$ , sham vs. smoke inhalation injury and  $p < 0.0001$ , sham vs. smoke + third-degree skin burn injury). There was a significant decrease in the percent normal blood vessels between the smoke inhalation injury and the combined smoke + third-degree skin burn group ( $p < 0.0001$ ). This same trend continued in the basal ganglia (**Figure 4B**) where there was a significant decrease in the percent normal blood vessels following smoke inhalation and the combined smoke + third-degree skin burn ( $p < 0.0001$  for sham vs. both injury groups). The decrease was also observed between the two injury groups with the decrease being most significant in the combined smoke + third-degree skin burn injury group ( $p < 0.0001$ , smoke inhalation injury vs. smoke + third-degree skin burn injury). The amygdala (**Figure 4B**) had a decrease in the percent total normal blood vessels in the smoke and the combined smoke + third-degree skin burn ( $p < 0.001$ , sham vs. smoke inhalation injury and  $p < 0.0001$ , sham vs. smoke + third-degree skin burn injury). The decrease in the percent normal blood vessels was observed between the smoke inhalation injury and the combined smoke + third-degree skin burn injury group ( $p < 0.001$ ), with the combined group showing the largest decrease. The decrease in normal blood vessels was seen in the hippocampus (**Figure 4B**) after the smoke inhalation injury and the combined smoke + third-degree skin burn ( $p < 0.001$ , sham vs. smoke inhalation injury and  $p < 0.0001$ , sham vs. smoke + third-degree skin burn injury). The decrease in the percent of normal blood vessels in the combined smoke + third-degree skin burn group ( $p < 0.05$ , smoke inhalation injury vs. smoke + third-degree skin burn injury) was statistically less than the smoke inhalation injury. In the cerebellum, there was a significant decrease in the percent normal blood vessels after the smoke and combined smoke + third-degree skin burn ( $p < 0.01$ , sham vs. smoke inhalation

injury and  $p < 0.0001$ , sham vs. smoke + third-degree skin burn injury). The decrease in the percent normal blood vessels was also observed between the smoke inhalation injury and the combined smoke + third-degree skin burn group ( $p < 0.01$ ), with the combined injury with the least normal blood vessels.

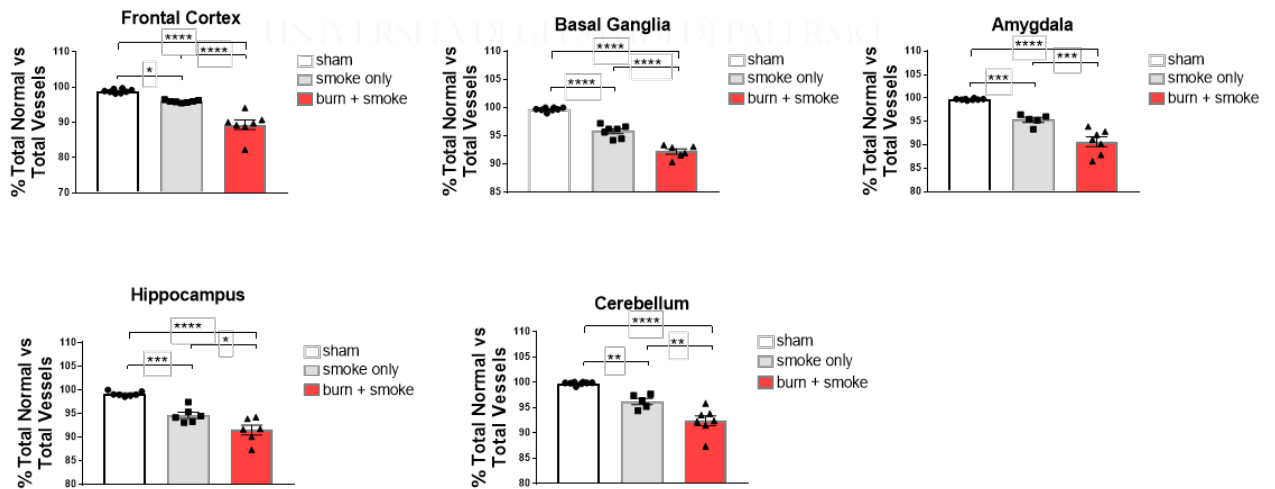


Figure 4B: Smoke inhalation ± third-degree skin burn caused a significant decrease in the total percent of normal blood vessels throughout the brain.

Data are shown as mean ± SEM of 10 representative areas of each brain region of interest. One-way ANOVA with Tukey's multiple comparison tests; \*  $p < 0.05$ , \*\*  $p < 0.01$ , \*\*\*  $p < 0.001$ , \*\*\*\*  $p < 0.0001$ .

**SMOKE INHALATION INJURY ± THIRD-DEGREE SKIN BURN RESULTED IN THE INCREASE OF THE PERCENT TOTAL DILATED VESSELS VS. TOTAL BLOOD VESSELS THROUGHOUT THE BRAIN.**

We determined if there was an increase in vessels that became dilated and congested following injury in the brain regions of interest. In the frontal cortex (**Figure 4C**), there was a significant increase in total dilated vessels between sham and the

combined smoke + third-degree skin burn injury group ( $p < 0.0001$ , sham vs. smoke + third-degree skin burn injury). There was also a significant increase between the two injury groups ( $p < 0.001$ , smoke inhalation injury vs. smoke + third-degree skin burn injury), with the combined injury group showing the highest increase in the percent of dilated and congested blood vessels for that region. The basal ganglia (**Figure 4C**) showed a significant percent increase in dilated and congested blood vessels after injury ( $p < 0.0001$  for sham vs. both injury groups). Dilated and congested blood vessels were also significantly more numerous in the combined injury group as compared to the smoke inhalation injury group ( $p < 0.0001$ , smoke inhalation injury vs. smoke + third-degree skin burn injury). There was a significant increase in the percent of dilated and congested vessels in the amygdala (**Figure 4C**) in the injury groups as compared to sham ( $p < 0.01$ , sham vs. smoke inhalation injury and  $p < 0.0001$ , sham vs. smoke + third-degree skin burn injury). There was also a significant increase in dilated and congested blood vessels between the smoke inhalation injury group as compared to the combined smoke + third-degree skin burn injury group ( $p < 0.001$ ). The same was observed in the hippocampus (**Figure 4C**) with a significant increase between sham and both injury groups ( $p < 0.01$ , sham vs. smoke inhalation injury and  $p < 0.0001$ , sham vs. smoke + third-degree skin burn injury). The increase in dilated and congested vessels was significant between the injury groups ( $p < 0.05$ , smoke inhalation injury vs. smoke + third-degree skin burn injury) with the combined group being the highest. The cerebellum (**Figure 4C**) showed a significant increase in the percent of dilated and congested blood vessels in the smoke inhalation injury and the combined smoke + third-degree skin burn groups ( $p < 0.0001$ , sham vs. both injury groups). The combined smoke + third-degree skin burn group had significantly

higher percent dilated and congested blood vessels as compared to the smoke inhalation only injury group ( $p < 0.001$ ).

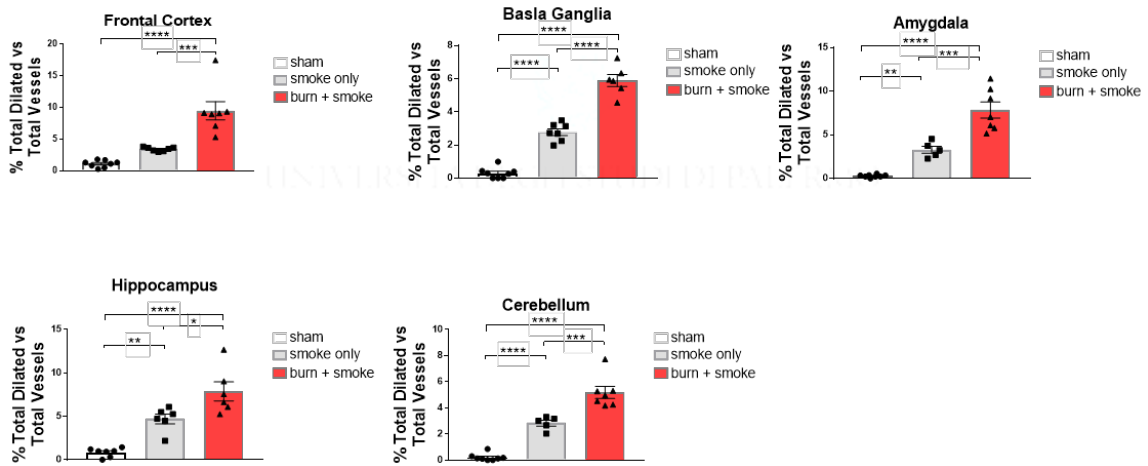


Figure 4C: Smoke inhalation  $\pm$  third-degree skin burn resulted in an increase of dilated blood vessels versus total vessels throughout the brain.

Data are shown as mean  $\pm$  SEM of 10 representative areas of each brain region of interest. One-way ANOVA with Tukey's multiple comparison tests; \*  $p < 0.05$ , \*\*  $p < 0.01$ , \*\*\*  $p < 0.001$ , \*\*\*\*  $p < 0.0001$ .

#### **THE INTEGRITY OF BLOOD VESSELS BASEMENT MEMBRANE IS LOST FOLLOWING SMOKE INHALATION INJURY $\pm$ THIRD-DEGREE SKIN BURN.**

To determine if the dilated and congested blood vessels seen in figure 3 were damaged following injury, we examined the integrity of the basement membrane using the PAS staining. The PAS stain is used to detect polysaccharides, such as glycogen, glycoproteins, and glycolipids. The basement membranes of blood vessels are composed of several polysaccharides and glycoproteins such as perlecan, fibronectin, and dystroglycan. Once blood vessels are damaged, the glycoproteins of the perlecan,

fibronectins, and dystroglycan are accessible for reaction with the Schiff reagent by damaged areas of the blood vessel showing a purple-magenta coloring.

There was a significant increase in damaged blood vessels following injury in the frontal cortex (**Figure 5**) following smoke inhalation injury and combined smoke + third-degree skin burn ( $p < 0.0001$ , sham vs. smoke inhalation injury and  $p < 0.001$ , sham vs. smoke + third-degree skin burn injury). The basal ganglia (**Figure 5**) also displayed damaged blood vessels in both injured groups compared to sham ( $p < 0.0001$ , sham vs. smoke inhalation injury and  $p < 0.001$ , sham vs. smoke + third-degree skin burn injury). The smoke inhalation injury group displayed a slightly higher level of damaged blood vessels than the combined smoke + third-degree burn group. There was an increase in the amygdala (**Figure 5**) between sham and injury groups ( $p = 0.0862$ , sham vs. smoke inhalation injury and  $p < 0.001$ , sham vs. smoke + third-degree skin burn injury), with the combined smoke + third-degree skin burn group having the highest increase in blood vessel damage. There was also a significant increase in damaged blood vessels between the smoke inhalation injury and the smoke + third-degree skin burn injury group ( $p < 0.05$ , smoke inhalation injury vs. smoke + third-degree skin burn injury). The hippocampus (**Figure 5**) showed an increase in the number of vessels that were damaged following dilation and congestion in both injury groups ( $p < 0.001$ , sham vs. smoke inhalation injury and  $p < 0.01$ , sham vs. smoke + third-degree skin burn injury) with the smoke inhalation injury group being slightly higher than the combined. The smoke inhalation injury group ( $p < 0.0001$ , sham vs. smoke inhalation injury) continued to have more damaged blood vessels than the combined smoke + third-degree skin burn group ( $p < 0.001$ , sham vs. smoke + third-degree skin burn injury) when compared to sham in the pons (**Figure 5**).

The increase in damaged blood vessels was most significant in the smoke inhalation injury group ( $p < 0.0001$ , sham vs. smoke inhalation injury) followed by the combined smoke + third-degree skin burn group ( $p < 0.001$ , sham vs. smoke + third-degree skin burn injury) in the cerebellum (**Figure 5**). In the pituitary gland (**Figure 5**), the combined smoke + third-degree skin burn group was statistically significant ( $p < 0.05$ , sham vs. smoke + third-degree skin burn injury) increase in damaged blood vessels.



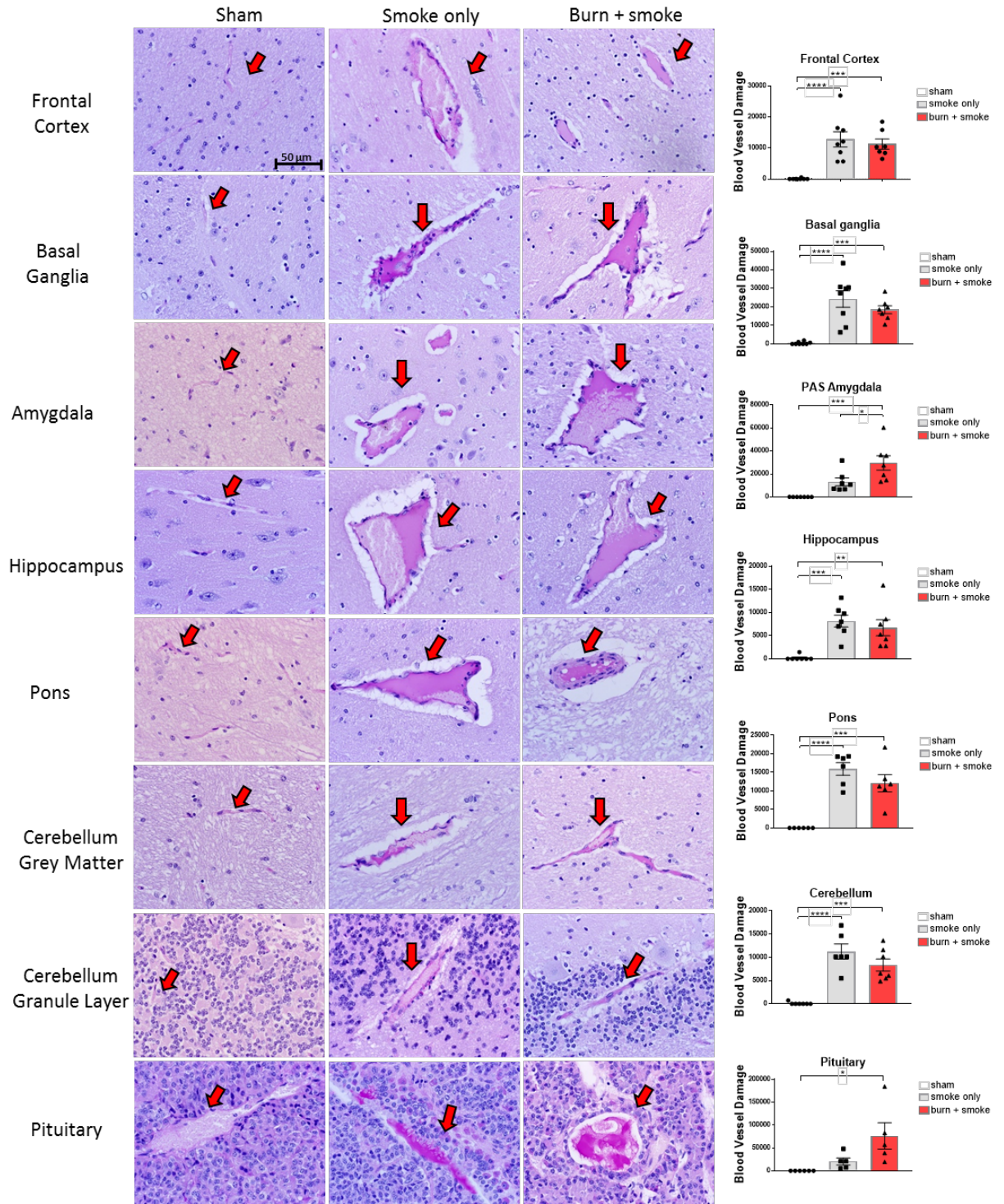


Figure 5: Confirmation of BBB dysfunction following smoke inhalation ± third-degree skin burn by positive PAS staining.

The integrity of the basement membranes of congested and dilated blood vessels was evaluated by staining with PAS. Once blood vessels are damaged, the glycoproteins of the perlecan, fibronectins, and dystroglycan are accessible for reaction with the Schiff reagent with damaged areas of the blood vessel showing a purple-magenta coloring. Following injuries, the congested and dilated blood vessels in the frontal cortex, basal ganglia, amygdala, hippocampus, pons, cerebellum grey matter, cerebellum granule layer, and pituitary gland were positive for PAS staining denoted by the red arrows. Data are shown as mean  $\pm$  SEM of 10 representative areas of each brain region of interest. One-way ANOVA with Tukey's multiple comparison tests; \*  $p < 0.05$ , \*\*  $p < 0.01$ , \*\*\*  $p < 0.001$ , \*\*\*\*  $p < 0.0001$ . Representative images of sheep brain coronal sections stained with PAS (calibration bar = 50  $\mu$ m).

#### **SMOKE INHALATION INJURY $\pm$ THIRD-DEGREE SKIN BURN RESULTED IN DILATED BLOOD VESSELS THAT RUPTURED IN THE BRAIN.**

The LFB/H&E revealed numerous congested and dilated vessels (**Figure 3**) that ruptured. In the frontal cortex (**Figure 6**), there was an increase in ruptured vessels following the smoke inhalation injury ( $p = 0.0715$ , sham vs. smoke inhalation injury). There was a significant increase in the number of ruptured vessels in the combined smoke + third-degree skin burn as compared to sham ( $p < 0.05$ , sham vs. smoke + third-degree skin burn injury). The basal ganglia (**Figure 6**) showed a significant increase in the number of ruptured vessels in both injury groups ( $p < 0.0001$ , sham vs. smoke inhalation injury and  $p < 0.001$ , sham vs. smoke + third-degree skin burn injury). Ruptured vessels in the amygdala (**Figure 6**) were significantly more following smoke inhalation injury ( $p < 0.001$ , sham vs. smoke inhalation injury) and smoke + third-degree skin burn



( $p < 0.001$ , sham vs. smoke + third-degree skin burn injury) as compared to sham. There was a significant increase of ruptured vessels in the hippocampus (**Figure 6**) after smoke inhalation injury ( $p = 0.0518$ , sham vs. smoke inhalation injury) as compared to sham. Following smoke inhalation injury ( $p = 0.0928$ , sham vs. smoke inhalation injury) in the cerebellum (**Figure 6**), there was an increase in ruptured vessels observed. The combined smoke + third-degree skin burn group ( $p < 0.01$ , sham vs. smoke + third-degree skin burn injury) had a significant increase in ruptured vessels as compared to sham.

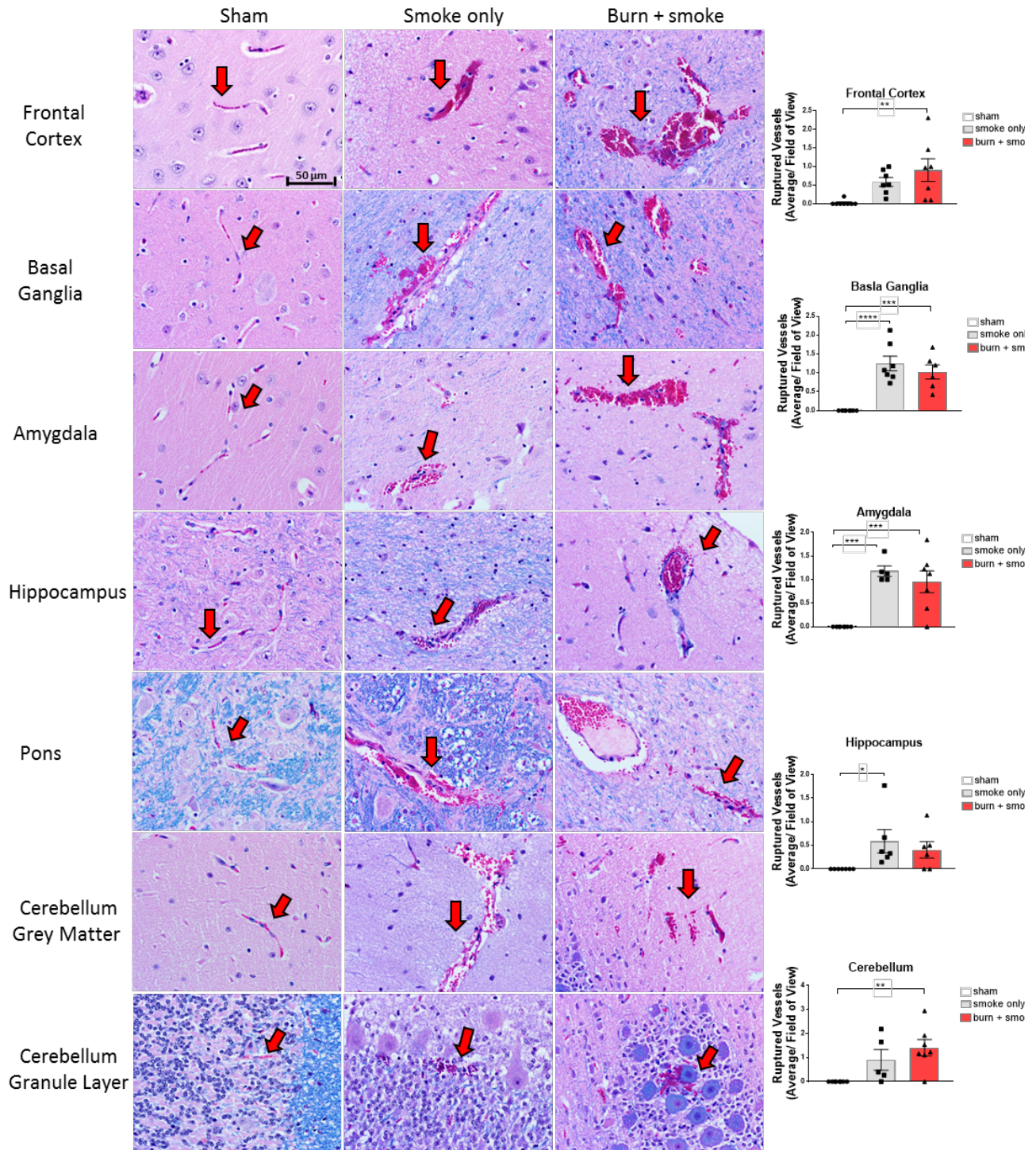


Figure 6: Luxol fast blue/ H&E staining revealed smoke inhalation ± third-degree skin burn caused BBB dysfunction characterized by congested and dilated blood vessels that ruptured throughout the brain.

Following smoke inhalation ± third-degree skin burn, vessels became congested with RBCs, dilated and ruptured in the frontal cortex, basal ganglia, amygdala, hippocampus, pons, cerebellum grey matter, and cerebellum granule layer. The red arrows denote the ruptured blood vessels. Data are shown as mean ± SEM of 10 representative areas of each brain region of interest. One-way ANOVA with Tukey's multiple comparison tests; \* p<0.05, \*\* p<0.01, \*\*\* p<0.001, \*\*\*\* p<0.0001. Representative images of sheep brain coronal sections stained with luxol fast blue (LFB) and counterstained with H&E (calibration bar = 50 mm).

**SMOKE INHALATION INJURY ± THIRD-DEGREE SKIN BURN RESULTED IN AN INCREASE IN THE PERCENT OF RUPTURED BLOOD VESSELS IN THE BRAIN.**

We determined if there was an increase in total vessels that rupture following injury in brain regions of interest. In the frontal cortex (**Figure 7A**), there was an increase in the percent total ruptured vessels compared to sham following the combined third-degree skin burn groups (p<0.01, sham vs. smoke + third-degree skin burn injury). There was a significant increase in the percent total vessels that rupture in the basal ganglia (**Figure 7A**) following smoke inhalation injury and the combined smoke + third-degree skin burn (p<0.001, sham vs. smoke inhalation injury and p<0.0001, sham vs. smoke + third-degree skin burn injury). The increase in the percentage of the total ruptured vessels was observed in the amygdala (**Figure 7A**) following smoke inhalation injury and the combined smoke + third-degree skin burn (p<0.01, sham vs. smoke inhalation injury and p<0.001, sham vs. smoke + third-degree skin burn injury). In the hippocampus (**Figure 7A**) there was an increase in the percent total ruptured vessels in both injury

groups. The increase following smoke inhalation injury was significant ( $p=0.0973$ , sham vs. smoke inhalation injury) as compared to sham. In the cerebellum (**Figure 7A**) there was an increase in the percent of total ruptured vessels following smoke inhalation injury. The increase was significant following the combined smoke + third-degree skin burn injury group ( $p<0.001$ , sham vs. smoke + third-degree skin burn injury).

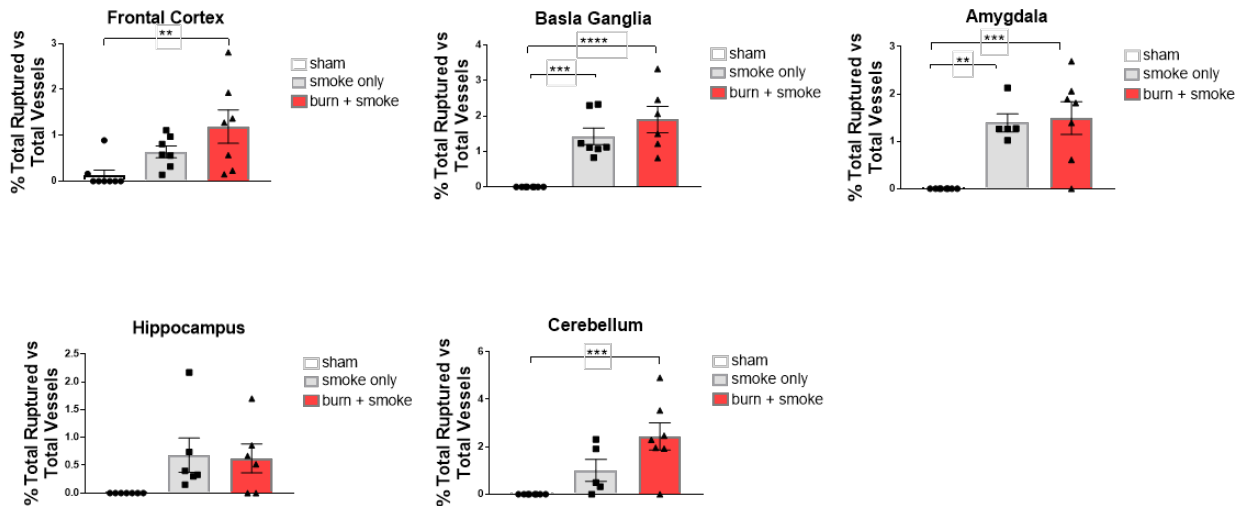


Figure 7A: Smoke inhalation  $\pm$  third-degree skin burn caused an increase in the percent total ruptured versus total blood vessels throughout the brain.

Data are shown as mean  $\pm$  SEM of 10 representative areas of each brain region of interest. One-way ANOVA with Tukey's multiple comparison tests; \*  $p<0.05$ , \*\*  $p<0.01$ , \*\*\*  $p<0.001$ , \*\*\*\*  $p<0.0001$ .

### SMOKE INHALATION INJURY CAUSED AN INCREASE IN DILATED VESSELS THAT RUPTURED IN THE BRAIN.

We examined how many of the dilated vessels ruptured following smoke inhalation injury and the combined smoke + third-degree skin burn. The percent of total

ruptured blood vessels that were dilated increased in the frontal cortex (**Figure 7B**) following smoke inhalation injury and the combined smoke + third-degree skin burn ( $p < 0.01$ , sham vs. smoke inhalation injury and  $p < 0.05$ , sham vs. smoke + third-degree skin burn injury). There was a significant increase in the percent total ruptured vessels that were dilated in the basal ganglia (**Figure 7B**) after smoke inhalation injury ( $p < 0.0001$ , sham vs. smoke inhalation injury and  $p < 0.001$ , sham vs. smoke + third-degree skin burn injury). There was a significant increase in the percent total ruptured vessels between the injury groups ( $p < 0.05$ , smoke inhalation vs. smoke inhalation + third-degree skin burn) with the combined smoke + third-degree skin burn higher than the smoke inhalation injury. There was a similar trend in the amygdala (**Figure 7B**) with an increase in ruptured blood vessels in the smoke inhalation and the combined smoke + third-degree skin burn groups ( $p < 0.0001$ , sham vs. smoke inhalation injury and  $p < 0.01$ , sham vs. smoke + third-degree skin burn injury). There was also a significant increase in ruptured blood vessels in the combined smoke + third-degree skin burn group as compared to the smoke inhalation injury group ( $p < 0.01$ , smoke inhalation injury vs. smoke + third-degree skin burn injury). In the hippocampus (**Figure 7B**) there was a significant increase in the percent total ruptured vessels versus total vessels following smoke inhalation injury ( $p < 0.05$ , sham vs. smoke inhalation injury). There was an increase following the combined smoke + third-degree skin burn. However, the increase was not statistically significant. The increase in the percent total ruptured vessels was significant after the smoke inhalation injury and the combined smoke + third-degree skin burn ( $p < 0.05$ , sham vs. smoke inhalation injury and  $p < 0.01$ , sham vs. smoke + third-degree skin burn injury) in the cerebellum (**Figure 7B**).

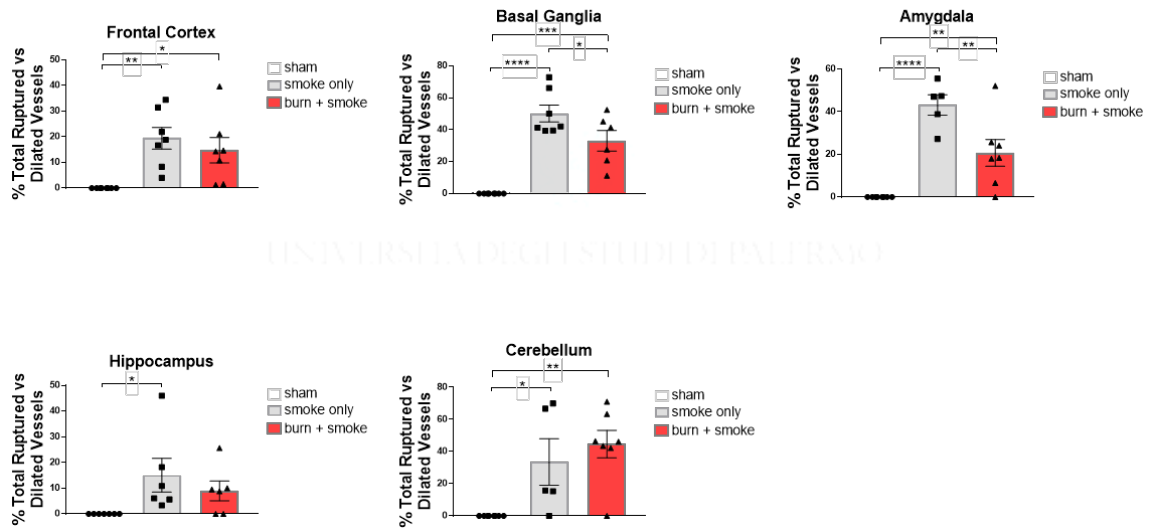


Figure 7B: Smoke inhalation ± third-degree skin burn caused an increase in the congested and dilated blood vessels in the brain that ruptured.

Data are shown as mean ± SEM of 10 representative areas of each brain region of interest. One-way ANOVA with Tukey's multiple comparison tests; \*  $p < 0.05$ , \*\*  $p < 0.01$ , \*\*\*  $p < 0.001$ , \*\*\*\*  $p < 0.0001$ .

### **SMOKE INHALATION INJURY ± THIRD-DEGREE SKIN BURN RESULTED IN MICROHEMORRHAGING IN THE BRAIN.**

LFB/ H&E staining showed severe microhemorrhaging following smoke inhalation ± third-degree skin burn (Figure 8). The frontal cortex demonstrated a significant increase in microhemorrhaging following smoke inhalation injury and the combined smoke + third-degree skin burn ( $p < 0.01$ , sham vs. smoke inhalation injury and  $p < 0.01$ , sham vs. smoke + third-degree skin burn injury). This trend was observed in the basal ganglia (Figure 8) with a significant increase in microhemorrhage following smoke



inhalation injury and smoke + third-degree skin burn ( $p < 0.01$ , sham vs. smoke inhalation injury and  $p < 0.01$ , sham vs. smoke + third-degree skin burn injury). There was an increase in microhemorrhaging in the amygdala (**Figure 8**) following smoke inhalation injury and the combined skin + third-degree skin burn. These increases, however, were not statistically significant. In the hippocampus (**Figure 8**), there was a significant increase in microhemorrhaging following smoke inhalation injury ( $p < 0.05$ , sham vs. smoke inhalation injury). There was a slight increase in microhemorrhaging following the combined smoke + third-degree skin burn injury. The cerebellum (**Figure 8**) displayed an increase in microhemorrhage following smoke inhalation injury. There was an increase in microhemorrhage in the combined smoke + third-degree skin burn group ( $p = 0.0550$ , sham vs. smoke + third-degree skin burn injury) following injury as compared to sham. The pituitary is a glandular tissue. Therefore, it was difficult to distinguish the area of individual microbleeds. Consequently, we measured the total RBCs in the tissue (Figure 8). There was a significant increase in total RBCs in the pituitary following smoke inhalation injury and the combined smoke + third-degree skin burn ( $p < 0.05$ , sham vs. smoke inhalation injury and  $p < 0.05$ , sham vs. smoke + third-degree skin burn injury).

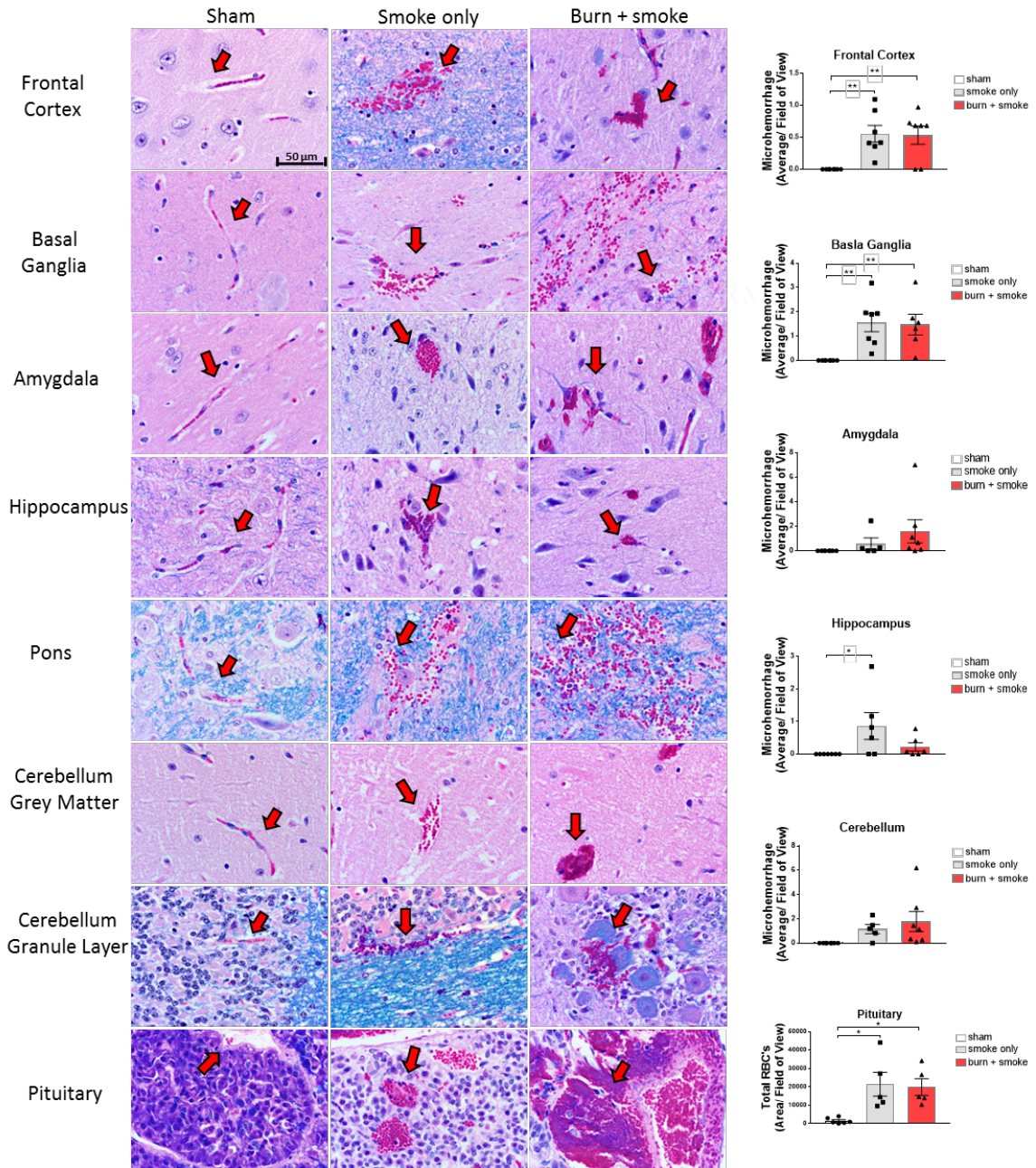


Figure 8: Luxol fast blue/ H&E staining reveals smoke inhalation ± third-degree skin burn resulted in microhemorrhaging throughout the brain.

Following smoke inhalation ± third-degree skin burn, there was significant microhemorrhaging in the frontal cortex, basal ganglia, amygdala, hippocampus, pons, cerebellum grey matter, cerebellum granule layer, and pituitary gland. The red arrows



denote the microhemorrhaging. Data are shown as mean  $\pm$  SEM of 10 representative areas of each brain region of interest. One-way ANOVA with Tukey's multiple comparison tests; \*  $p < 0.05$ , \*\*  $p < 0.01$ , \*\*\*  $p < 0.001$ , \*\*\*\*  $p < 0.0001$ . Representative images of sheep brain coronal sections stained with luxol fast blue (LFB) and counterstained with H&E (calibration bar = 50  $\mu$ m).

#### **CONFIRMATION OF MICROHEMORRHAGING FOLLOWING SMOKE INHALATION INJURY $\pm$ THIRD-DEGREE SKIN BURN BY POSITIVE MSB STAINING.**

To further characterize the microhemorrhaging observed in the LFB/H&E staining, we analyzed fibrin(ogen) deposition into the brain parenchyma using MSB staining (Figure 9). Fibrin is a 340-kD macromolecule normally excluded from the brain. Entry into the brain parenchyma results in increased neurovascular damage, neuroinflammation, neuronal degeneration, and cognitive decline (45, 46).

There was an increase in fibrin(ogen) deposition in the frontal cortex (**Figure 9**) following smoke inhalation injury with the most significant increase in the smoke + third-degree skin burn injury group ( $p < 0.001$ , sham vs. smoke + third-degree skin burn injury) as compared to sham. There was a significant increase in fibrin(ogen) deposition between the injury groups, with the combined injury being most severe ( $p < 0.05$ , smoke inhalation injury vs. smoke + third-degree skin burn injury). This same trend was observed in the basal ganglia (**Figure 9**), where there was a slight increase in fibrin(ogen) deposition in the smoke inhalation group. The smoke + third-degree skin burn group showed a significant increase compared to sham ( $p < 0.01$ ; sham vs. smoke + third-degree skin burn injury) and a significant increase as compared to the smoke only group ( $p < 0.05$ , smoke

inhalation injury vs. smoke + third-degree skin burn injury). In the amygdala (**Figure 9**), both injury groups showed an increase in fibrin(ogen) deposition as compared to sham ( $p < 0.01$ , sham vs. smoke inhalation injury and  $p < 0.001$ , sham vs. smoke + third-degree skin burn injury). There was an increase in fibrin(ogen) deposition in the hippocampus (**Figure 9**) following injury. However, the increase was not significant in either injury group as compared to sham or between both injury groups ( $p = 0.0655$ , sham vs. smoke inhalation injury and  $p = 0.1010$ , sham vs. smoke + third-degree skin burn injury). In the pons (**Figure 9**), there was a significant increase in fibrin(ogen) in the brain following the smoke inhalation injury and the smoke + third-degree skin burn ( $p = 0.05$ , sham vs. smoke inhalation injury and  $p < 0.01$ , sham vs. smoke + third-degree skin burn injury). The smoke only group in the cerebellum (**Figure 9**) resulted in an increase in fibrin(ogen) deposition following injury, and the combined smoke + third-degree skin burn ( $p < 0.01$ , sham vs. smoke + third-degree skin burn injury) showed a significant increase as compared to sham. In the pituitary (**Figure 9**), there was an increase in fibrin(ogen) deposition following smoke inhalation injury. There was a significant increase in the smoke + burn group ( $p < 0.0001$ , sham vs. smoke + third-degree skin burn injury) as compared to sham and between both injuries ( $p < 0.01$ , smoke inhalation injury vs. smoke + third-degree skin burn injury).

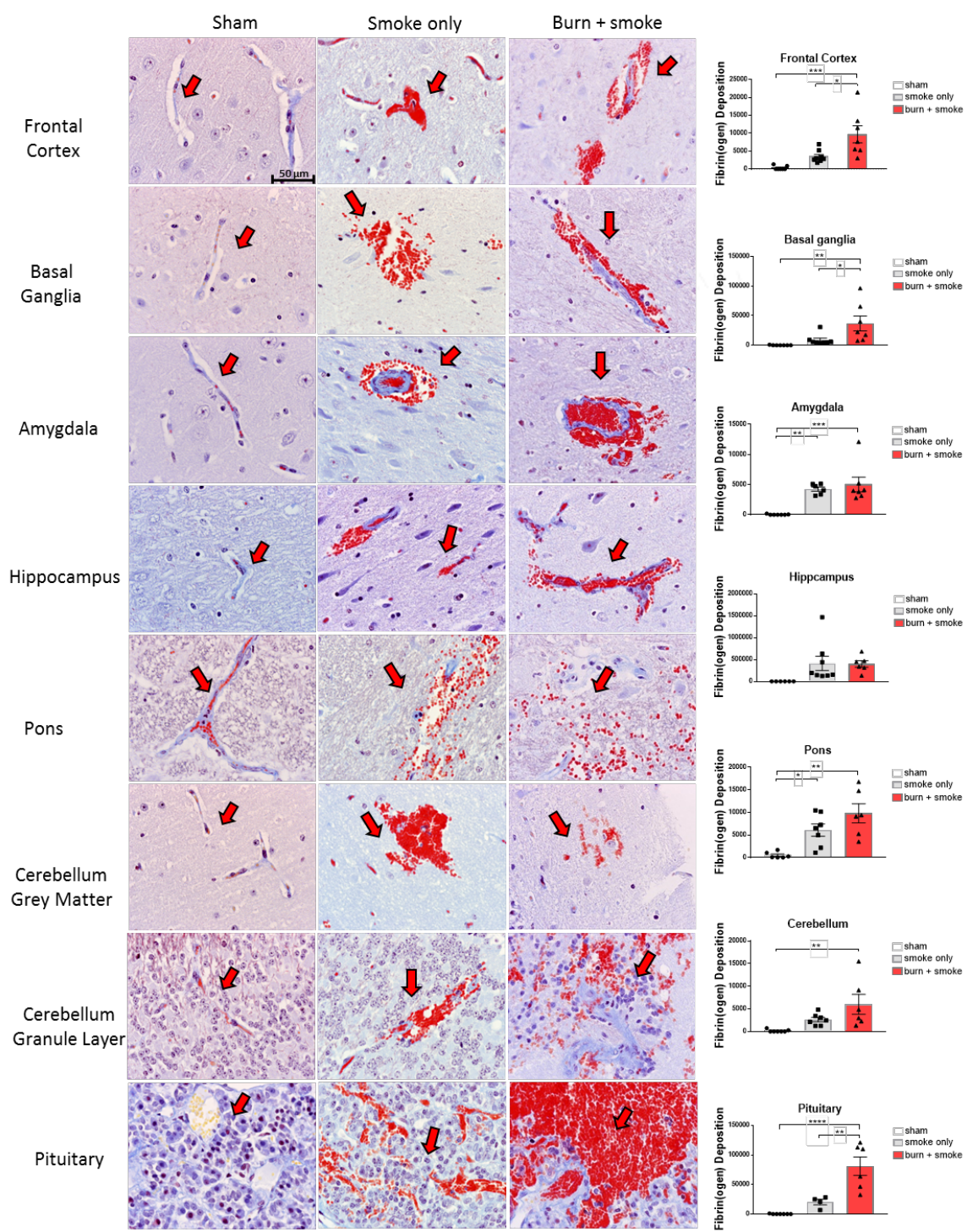


Figure 9: Confirmation of microhemorrhaging following smoke inhalation ± third-degree skin burn by positive MSB staining throughout the brain.

To confirm neurovascular dysfunction of the BBB, MSB detected fibrin(ogen) deposition into brain tissue demonstrated by a cherry red coloring. Fibrin is a 340-kD macromolecule normally excluded from the brain. Following injuries, there was positive MSB staining of fibrin(ogen) in the frontal cortex, basal ganglia, amygdala, hippocampus, pons, cerebellum grey matter, cerebellum granule layer, and pituitary gland. The red arrows denote positive MSB staining. Data are shown as mean ± SEM of 10 representative areas of each brain region of interest. One-way ANOVA with Tukey's multiple comparison tests; \*  $p < 0.05$ , \*\*  $p < 0.01$ , \*\*\*  $p < 0.001$ , \*\*\*\*  $p < 0.0001$ . Representative images of sheep brain coronal sections stained with MSB (calibration bar = 50 mm).

**SMOKE INHALATION INJURY ± THIRD-DEGREE SKIN BURN RESULTED IN BBB DYSFUNCTION IN THE BRAIN CONFIRMED BY POSITIVE ALBUMIN STAINING.**

Immunohistochemistry was used to assess BBB dysfunction by examining albumin extravasation in the brain parenchyma (**Figure 10**). In all brain regions examined, there was an increase in albumin staining in the smoke inhalation injury and the combined smoke + third-degree skin burn groups. Specifically, in the frontal cortex, there was a significant increase in albumin deposition following the combined smoke + third-degree skin burn ( $p < 0.05$ , sham vs. smoke + third-degree skin burn injury). In the basal ganglia, there was a significant increase in albumin deposition following the combined smoke + third-degree skin burn ( $p < 0.01$ , sham vs. smoke + third-degree skin

burn injury). Additionally, there was a significant increase in albumin deposition in the smoke + third-degree skin burn group as compared to smoke inhalation injury ( $p < 0.05$ , smoke inhalation injury vs. smoke + third-degree skin burn injury). The albumin staining increased following the combined smoke + third-degree skin burn, however the increase was not significant. In the hippocampus, there was an increase in albumin following smoke inhalation and smoke + third-degree skin burn injuries. The increase in the hippocampus was not significant. The cerebellum had an increase in albumin staining following both injuries in the cerebellum ( $p < 0.05$ , sham vs. smoke inhalation injury and  $p < 0.05$ ; sham vs. smoke + third-degree skin burn injury) as compared to sham. There was an increase in albumin following both injuries in the pituitary gland, with the combined injury of smoke + third-degree skin burn being the highest. However, these increase were not significant in either groups due to variability. This same trend was also observed in the pons.

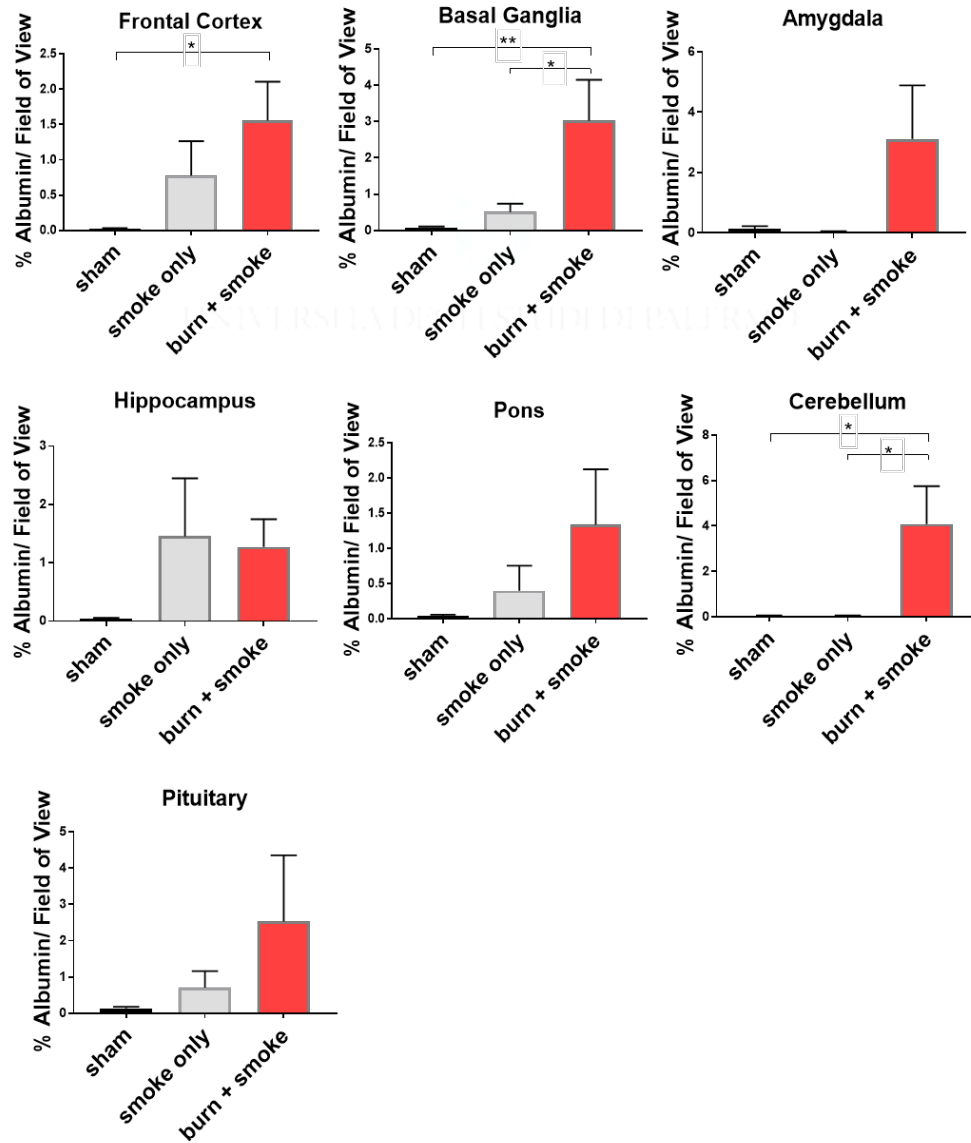


Figure 10: Smoke inhalation ± third-degree skin burn resulted in microhemorrhaging in the brain confirmed by positive albumin staining.

Smoke inhalation ± third-degree skin burn, results in albumin extravasation in the frontal cortex, basal ganglia, amygdala, hippocampus, pons, cerebellum grey matter, cerebellum granule layer, and pituitary gland confirming BBB dysfunction. Data are shown as mean

± SEM of 10 representative areas of each brain region of interest. One-way ANOVA with Tukey's multiple comparison tests; \*  $p < 0.05$ , \*\*  $p < 0.01$ , \*\*\*  $p < 0.001$ , \*\*\*\*  $p < 0.0001$ .

### **SMOKE INHALATION INJURY ± THIRD-DEGREE SKIN BURN RESULTED IN NEUTROPHIL INFILTRATION IN THE BRAIN.**

Neutrophil infiltration was observed in all regions of interest in the LFB/H&E staining (**Figure 11**). In the frontal cortex there was a significant increase in neutrophils following smoke inhalation injury ( $p < 0.01$ , sham vs. smoke inhalation injury). There was an increase in neutrophil infiltration following smoke + third-degree skin burn injury, however the increase was not statistically significant. There was an increase in neutrophil infiltration in the basal ganglia (**Figure 11**) following both injuries. However, the increase observed in both injury groups was not significant. In the amygdala (**Figure 11**), there was an increase in neutrophils in the smoke inhalation injury as compared to sham. There was a significant increase in neutrophil infiltration after the combined smoke + third-degree burn group ( $p < 0.05$ , sham vs. smoke + third-degree skin burn). The increase in neutrophils in the hippocampus (**Figure 11**) was the highest following the smoke inhalation injury group. The combined smoke + third-degree skin burn group had a slight increase in neutrophil infiltration. The increase in neutrophils in the hippocampus was not significant in either injury group. Neutrophil infiltration was increased in the cerebellum (**Figure 11**) after smoke inhalation injury only and the combined smoke + third-degree skin burn. The increase in both groups was not statistically significant.



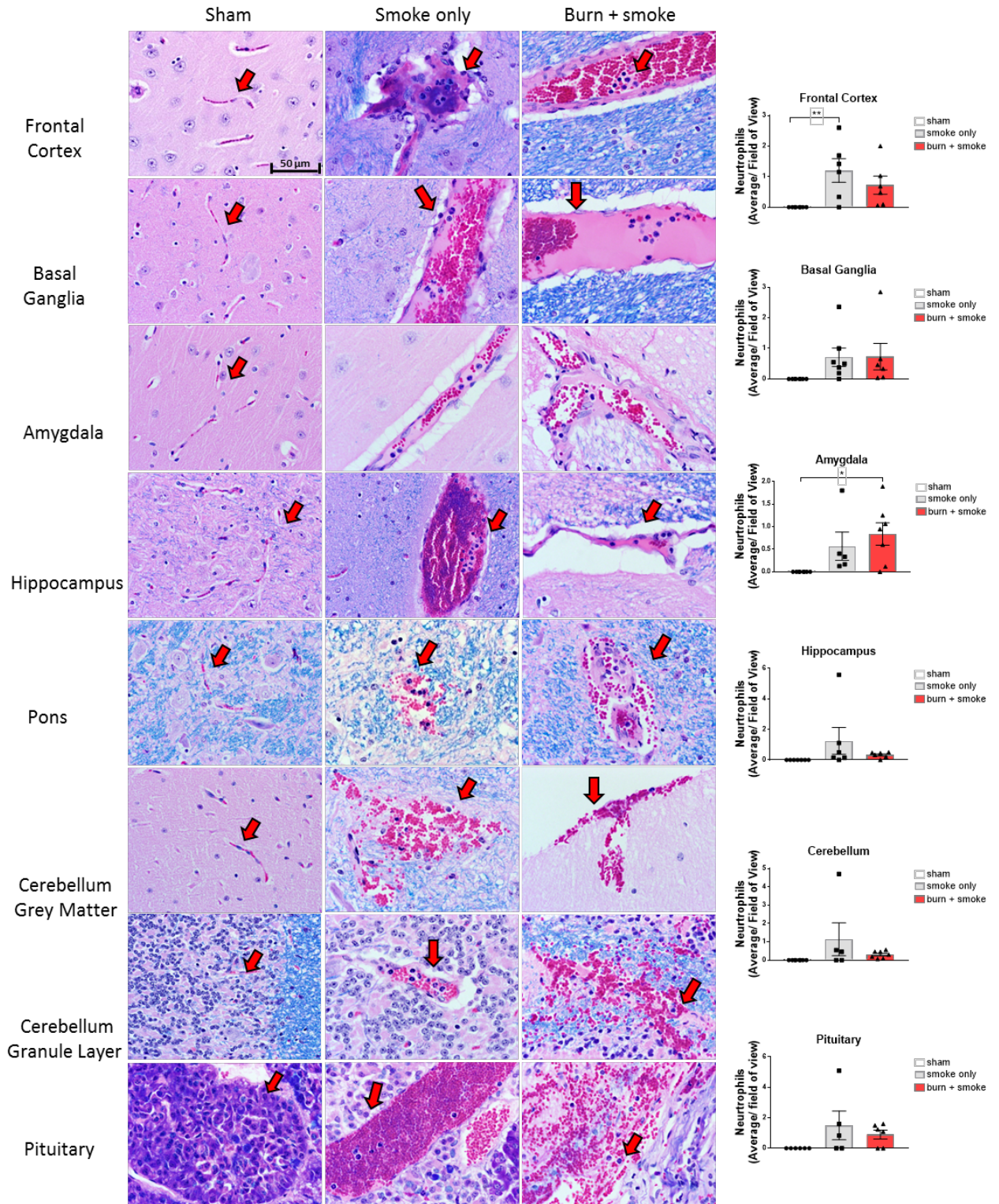




Figure 11: Smoke inhalation  $\pm$  third-degree skin burn resulted in neutrophil infiltration into the brain.

Following smoke inhalation  $\pm$  third-degree skin burn, congested and dilated blood vessels were infiltrated with neutrophils in the frontal cortex, basal ganglia, amygdala, hippocampus, pons, cerebellum grey matter, cerebellum granule layer, and pituitary gland. The red arrows denote the neutrophils. Data are shown as mean  $\pm$  SEM of 10 representative areas of each brain region of interest. One-way ANOVA with Tukey's multiple comparison tests; \*  $p < 0.05$ , \*\*  $p < 0.01$

## Chapter 4 Discussion

Although the pathophysiology of smoke inhalation-induced lung injury has been extensively studied, little is known about the acute and long-term effects of smoke inhalation on the CNS. As of today, two clinical reports have been published showing that CNS dysfunctions occur following smoke inhalation injury  $\pm$  third-degree skin burn. The nightclub fire in Brazil, suggest that neurological complications such as a persistent headache, memory loss, and paresthesia occur following smoke inhalation injury. Additionally, one case report concluded that acute smoke inhalation injury results in a long-term global decrease in metabolic activity and degeneration of several areas of the brain. It is important to stress that this case report is limited to only one patient. Clearly, CNS dysfunction following smoke inhalation  $\pm$  third-degree skin burn is a neglected field of investigation. Therefore, there is a huge gap in knowledge that must be filled to effectively treat patients who have suffered smoke inhalation  $\pm$  third-degree skin burn.

This is particularly important because recent advances in clinical care and the development of novel treatments have greatly increased the survival of burn injury and smoke inhalation injury patients, thus warranting the need for follow-up studies aimed at determining possible pathological alterations of the CNS and associated cognitive dysfunctions. We want to fill this gap.

Additionally, there are no postmortem studies to identify the underlying cause of CNS dysfunction following injury. Using a well-established ovine model, here we show for the first time that smoke inhalation, regardless of the presence of third-degree skin burn, leads to diffuse loss of blood-brain barrier integrity resulting in bleeding in the lateral ventricles, a reduction in normal blood vessels with concomitant increase in dilated and congested blood vessels, ruptured blood vessels, microhemorrhaging, and neutrophil infiltration in the brain parenchyma.

**SMOKE INHALATION INJURY ± THIRD-DEGREE SKIN BURN CAUSES BLEEDING IN THE LATERAL VENTRICLES AND MACROHEMORRHAGING THROUGHOUT THE BRAIN.**

We investigated the underlying cause of the neurological complications observed following acute smoke inhalation ± third-degree skin burn and found a potential link with the dysfunction of the BBB. Postmortem sheep brains following smoke inhalation ± third-degree skin burn revealed intraventricular hemorrhaging. In several postmortem sheep brains, the lateral ventricles were enlarged due to the accumulation of blood. In rare cases, the enlarged ventricles ruptured causing bleeding in the brain parenchyma (**Figure 1B**).

The sheep model has limitations in studying cognitive deficits; however, there are several studies demonstrating how intraventricular hemorrhaging can lead to several life-threatening complications. Specifically, intraventricular hemorrhaging can result in a decreased level in consciousness, particularly with hemorrhaging in the reticular activating system (the nuclei in the mesencephalon that control the three sleep and arousal states; waking, asleep, and asleep with dreaming) and in the thalamus (47, 48). Several randomized controlled stroke (brain hemorrhage) studies revealed bleeding in the lateral ventricles increases mortality by 50- 80%, decreases the level of consciousness, results in a poorer functional outcome, and increase morbidity (47). Additionally, stroke patients with intraventricular hemorrhaging are three times more likely to die than stroke patients without intraventricular hemorrhaging (47).

Also, there is a direct link between the volume of blood in the ventricles and the duration of coma (47, 49, 50). Moreover, intraventricular hemorrhaging results in blood clots that can block cerebrospinal fluid (CSF) limiting cerebral perfusion, resulting in obstructive (communicating) hydrocephalus. This contributes to the mass effect and cerebral edema in these patients (47). The breakdown of residual blood clots that are not cleared can cause permanent occlusion and scarring once embedded in the arachnoid granulations (47). Scarring of the arachnoid granulation limits CSF absorption resulting in nonobstructive (noncommunicating) hydrocephalus (47). The persistence of blood clots and blood breakdown products in the lateral ventricles cause decreased blood clot resolution due to the presence of coagulation and fibrinolytic pathways (47). The impaired clot resolution in the lateral ventricles leads to the accumulation of blood breakdown products, and consequently to an inflammatory reaction.

Previous studies using animal models of intraventricular hemorrhage demonstrated that such inflammatory reaction could affect long-term cognitive function (47, 49). These findings were supported by Hutter et al. who demonstrated significant deficits in neuropsychological testing in human patients with subarachnoid hemorrhage and intraventricular hemorrhaging as compared to patients without intraventricular hemorrhage (47, 51). Together with these findings, our data provide key insights that smoke inhalation ± third-degree skin burn can lead to cognitive deficits due to bleeding in the lateral ventricles.

**SMOKE INHALATION INJURY ± THIRD-DEGREE SKIN BURN CAUSES BBB DYSFUNCTION CHARACTERIZED BY CONGESTED AND DILATED BLOOD VESSELS THROUGHOUT THE BRAIN.**

Our data show that smoke inhalation ± third-degree skin burn results in blood vessels dilation in the brain contributing to microvascular dysfunction. The congestion of red blood cells (RBCs) in the lumen resulted in the severe dilation of arterial blood vessels in the frontal cortex, basal ganglia, amygdala, hippocampus, pons, cerebellum, and pituitary gland (**Figure 3**). The influx of RBCs into the blood vessels caused severe dilation leading to the damage of the blood vessels, which was confirmed by positive PAS staining (**Figure 5**). Positive PAS staining demonstrated damage to the blood vessels as a possible underlying cause of BBB dysfunction following smoke inhalation ± third-degree skin burn. There was also a significant reduction of normal blood vessels following injury in all brain regions of interest (**Figure 4**).

**SMOKE INHALATION INJURY ± THIRD-DEGREE SKIN BURN CAUSES BBB DYSFUNCTION CHARACTERIZED BY CONGESTED AND DILATED BLOOD VESSELS THAT RUPTURE THROUGHOUT THE BRAIN.**

Bleeding in the brain causes a series of deleterious events leading to secondary brain injuries such as inflammation, oxidative stress, hypermetabolism, excitotoxicity, and hematoma cytotoxicity (52). The microvascular dysfunction caused by the obstruction of the blood vessels leads to significant rupturing of blood vessels following smoke inhalation ± third-degree skin burn (**Figure 6**). Additionally, smoke inhalation injury alone causes rupturing of dilated vessels leading us to believe there is chemical(s) in the smoke that damages and weakens the blood vessels. The percent ruptured vessels versus total vessels were higher in the frontal cortex, basal ganglia, amygdala, and cerebellum (**Figure 7A**). The cerebellum was the only brain region of interest where the combined smoke + third-degree skin burn resulted in higher rupturing of dilated vessels. The percent ruptured vessels versus total dilated vessels were significantly higher in the frontal cortex, basal ganglia, amygdala, hippocampus, and cerebellum (**Figure 7B**).

Examining clinical symptoms of rupturing of blood vessels has shed light on similarities of observed cognitive dysfunction following smoke inhalation ± third-degree skin burn. For instance, clinical manifestation of bleeding in the frontal cortex is demonstrated in frontal lobe strokes.

Strokes confined to the basal ganglia present with a broad range of deficits depending on the location of the ruptured blood vessels (53). The basal ganglia are a group of subcortical nuclei comprised of the striatum, globus pallidus, subthalamic nuclei, and substantia nigra (53). Due to the high level of connectivity to different brain regions, the basal ganglia control a variety of functions such as control of motor

functions, limbic functions (emotions), and executive functions (attention, memory, implicit learning, and habit formation) (53). Several clinical studies demonstrated that bleeding in the basal ganglia is associated with significant reduction in motor weakness, attention, learning, language, executive and visuospatial functions (54, 55).

The hippocampus is the major consolidator of short-term memory into long-term memory. Bleeding in the hippocampus has been shown to result in memory impairment, difficulty in word finding, hemiparesis, and disturbances in memory, visual memory, and attention (56).

The pons, a component of the brain stem, plays a role in controlling respiratory function, sleep-wake cycle, and consciousness (57). Strokes in the pons are characterized by neurological deficits, respiratory failure, headache, vertigo, and disturbances of consciousness (58). Additionally, a clinical review of 78 patients with brainstem strokes by D'aes and Mariën reported patients suffered from impairment of limbic or cortical areas presenting as cognitive symptoms such as deficits in attention, executive function, intellectual capacity, memory, language, visuo-spatial skills (59).

Rupturing of blood vessels in the cerebellum (function in coordinated motor movement), or acute cerebellar infarctions, are associated with life-threatening neurological complications due to limitations of neurosurgery interventions (60). Acute cerebellar infarctions present with several clinical symptoms such as declining level of consciousness, coma, ataxia, headache, dysarthria, vertigo, poor balance, difficulty walking, obstructive hydrocephalus, and brain stem compression due to mass effect (60).

**SMOKE INHALATION INJURY ± THIRD-DEGREE SKIN BURN RESULTED IN MICROHEMORRHAGING THROUGHOUT THE BRAIN.**

The extravasation of RBCs and blood proteins into brain parenchyma was further exacerbated by microhemorrhaging following smoke inhalation ± third-degree skin burn (**Figure 8**). There was a significant increase in microhemorrhaging in the frontal cortex, basal ganglia, and the pituitary gland. In the amygdala and cerebellum, there was an increase in microhemorrhaging, with the combined smoke inhalation injury + third-degree skin burn having the highest increase.

Following large burns, patients suffer from a hypermetabolic response associated with a severely altered hormone profile due to hypothalamic-pituitary-organ axis dysfunction (34). During the acute phase of hypothalamic-pituitary-organ axis dysfunction, the pituitary gland is actively secreting hormones, however due to the development of target-organ resistance, peripheral hormone levels are low. The endocrine axis is suppressed by the hypothalamus during the long-term phase resulting in low peripheral hormone levels. Several clinical trials aimed to correct hormonal dysbalances following critical injuries were unsuccessful (34). Vanhorebeek et al., 2006 believed this failure was due to the lack of knowledge of the pathophysiological mechanism (61). Our data suggest, that changes in the hypothalamic-pituitary-organ axis dysfunction could be linked to microhemorrhaging in the pituitary gland.

**CONFIRMATION OF MICROHEMORRHAGING FOLLOWING SMOKE INHALATION INJURY ± THIRD-DEGREE SKIN BURN BY POSITIVE MSB STAINING THROUGHOUT THE BRAIN.**

Additionally, we used MSB staining (**Figure 8**) to confirm microhemorrhaging throughout the brain following injury. MSB detects fibrin(ogen), a 340-kD

macromolecule normally excluded from the brain. The frontal cortex, basal ganglia, and the pituitary gland had a significant increase in fibrin(ogen) in the brain following the combined smoke inhalation injury + third-degree skin burn. There was also a significant increase in fibrin(ogen) deposition when compared with smoke inhalation injury in these groups as well. The amygdala and the pons had a significant increase in fibrin(ogen) deposition between sham and both injury groups. In the cerebellum, the combined burn + third-degree skin burn injury group was significantly higher than the sham.

Entry of fibrin(ogen) into the brain parenchyma results in increased neurovascular damage, neuroinflammation, neuronal degeneration, and cognitive decline (45, 46). Several studies have demonstrated microhemorrhaging is associated with gait disturbances, cognitive impairment in many cognitive domains such as information processing, executive functions, and slower motor speeds (62, 63). Additionally, fibrin(ogen) deposition into the parenchyma has been shown to activate CNS innate and adaptive immune responses by interacting with the CD11b/CD18 integrin receptor on microglia, macrophages, and neutrophils (45, 64).

#### **SMOKE INHALATION INJURY ± THIRD-DEGREE SKIN BURN RESULTED IN NEUTROPHIL INFILTRATION THROUGHOUT THE BRAIN.**

Following smoke inhalation ± third-degree skin burn, there was an increase in granulated polymorphonuclear cells (PMNs), such as neutrophils, throughout the brain. Notably, in the frontal cortex, basal ganglia, hippocampus, cerebellum, and the pituitary gland a higher number of infiltrating neutrophils was present following smoke inhalation injury. Circulating neutrophils are the first to migrate to areas of infection or invading



microbes (65). We believe neutrophil infiltration is highest in this group because it is not being sequestered to the periphery due to third-degree skin burn. Additionally, the decrease in neutrophil infiltration following smoke + third-degree skin burn could be due to impairment of the immune system. Several studies have shown that large skin burns (30-40% TBSA) result in a profound hypermetabolic and inflammatory response resulting in the loss of lean body mass for up to 24 months post injury (34). Additionally, it was demonstrated by Cheng et al., impaired immune function occurs with a 10% decrease in body mass. We believe this could be the cause of the neutrophil reduction observed following the combined injury of smoke + third-degree skin burn.

## **Chapter 5 Conclusion**

In this thesis, I describe, for the first time that smoke inhalation alone or in combination with third-degree skin burn results in profound pathological changes in the brain that are not secondary to changes in hemodynamic parameters. Moreover, my results indicate that a well-characterized ovine model of smoke inhalation ± third-degree skin burn is not only a good model to investigate pulmonary pathophysiology, but also a useful model to elucidate acute damages to the CNS following smoke and burn injury.

In conclusion, my data demonstrate important pathological alterations in the CNS after smoke injury and lay the foundation for future studies aimed at further characterizing the contributing factors leading to progressive neurological deficits observed after acute exposure to smoke inhalation. My findings should have a high impact on the field because by identifying smoke inhalation ± third-degree skin burn as

an underlying cause for CNS dysfunction points to the need to include neurological examinations in the standard operating protocol for these patients.

## **Bibliography**

UNIVERSITÀ DEGLI STUDI DI PALERMO

1. Alcorta R. Smoke inhalation & acute cyanide poisoning. Hydrogen cyanide poisoning proves increasingly common in smoke-inhalation victims. *Journal of Emergency Medical Services* 2004;29(8):S6- S15.
2. Rehberg S, Maybauer MO, Enkhbaatar P, Maybauer DM, Yamamoto Y, Traber DL. Pathophysiology, management and treatment of smoke inhalation injury. *Expert Rev Respir Med.* 2009;3(3):283-97.
3. Martins de Albuquerque I, Schmidt Pasqualoto A, Trevisan ME, Pereira Goncalves M, Viero Badaro AF, Potiguara de Moraes J, et al. Role of physiotherapy in the rehabilitation of survivors of the Kiss nightclub tragedy in Santa Maria, Brazil. *Physiotherapy.* 2013;99(4):269-70.
4. (CDC) CfDCaP. Rapid assessment of injuries among survivors of the terrorist attack on the World Trade Center--New York City, September 2001. *Morbidity and Mortality Weekly Report.* 2002;51(1):1-5.
5. Schwela D. Cooking smoke: a silent killer. *People Planet.* 1997;6(3):24-5.
6. Enkhbaatar P, Pruitt BA, Suman O, Mlcak R, Wolf SE, Sakurai H, et al. Pathophysiology, research challenges, and clinical management of smoke inhalation injury. *The Lancet.* 2016;388(10052):1437-46.

7. Edward A. Bittner MD, Ph.D., F.C.C.M., Erik Shank, M.D., Lee Woodson, M.D., Ph.D., J. A. Jeevendra Martyn, M.D., F.R.C.A., F.C.C.M. <Acute and Perioperative Care of the Burn-injured Patient.pdf>. *Anesthesiology*. 2015;122(2):448-64.
8. Williams FN, Jeschke MG, Chinkes DL, Suman OE, Branski LK, Herndon DN. Modulation of the hypermetabolic response to trauma: temperature, nutrition, and drugs. *J Am Coll Surg*. 2009;208(4):489-502.
9. Woodson LC. Diagnosis and Grading of Inhalation Injury. *Journal of Burn Care & Research*. 2009;30(1):143-5.
10. Tanizaki S. Assessing inhalation injury in the emergency room. *Open Access Emergency Medicine*. 2015;7:31–7.
11. Clark WR BM, Myers W. Smoke inhalation and airway management at a regional burn unit: 1974-1983. Part I: Diagnosis and consequences of smoke inhalation. *Journal of burn Care and Rehabilitation*. 1989;10(1):52-62.
12. Preea Gill RVM. Smoke inhalation injury. *British Journal of Anaesthesia Education*. 2015;15(3):143-8.
13. Maybauer MOMDMMDNHDLTMO. The role of superoxide dismutase in systemic inflammation. *Shock*. 2006;25(2):206-7.
14. Bjerknes HVEUR. Increased Levels of Circulating Interleukin-8 in Patients with Large Burns: Relation to Burn Size and Sepsis. *The Journal of Trauma: Injury, Infection, and Critical Care* 1995;39(4):635-40.
15. RH D. Smoke inhalation lung injury: an update. *Eplasty*. 2008;8.
16. Fink MP. Role of reactive oxygen and nitrogen species in acute respiratory distress syndrome. *Current Opinion in Critical Care*. 2002;8(1):6-11.

17. Szabó DGC. Poly(ADP-ribose) polymerase: a new therapeutic target? *Current Opinion in Anaesthesiology*. 2008;21(2):111–21.
18. Szabo PPaC. Role of the Peroxynitrite-Poly(ADP-Ribose) Polymerase Pathway in Human Disease. *The American Journal of Pathology*. 2008;173(1):2–13.
19. Rehberg S MM, Maybauer DM, Traber LD, Enkhbaatar P, Traber DL. The role of nitric oxide and reactive nitrogen species in experimental ARDS. *Frontiers in Bioscience* 2010;1(2):18-29.
20. Association AB. 2015 National Burn Repository: Report of data from 2005-2014. <http://www.ameriburn.org>: American Burn Association 2015.
21. Deirdre Church SE, Owen Reid, Brent Winston, and Robert Lindsay. Burn Wound Infections. *Clinical Microbiology Reviews* 2006;19(2):403–34.
22. Scott DeBoer RN AmOCR. Prehospital and emergency department burn care. *Critical Care Nursing Clinics of North America*. 2004;16(1):61-73.
23. Dyer C RD. Thermal trauma. *The Nursing Clinics of North American* 1990;25(1):85-117.
24. <Handbooks of burns volume 1 .pdf>.
25. A. R. Moritz and F. C. Henriques J. Studies of Thermal Injury  
II. The Relative Importance of Time and Surface Temperature in the Causation of Cutaneous Burns. *American Journal of Pathology*. 1947;23(5):695-720.
26. Flynn M. Trauma nursing: from resuscitation through rehabilitation. K McQuillan KV, R Hartsock, M Flynn, E Whalen, editor. WB Saunders, Philadelphia: WB Saunders; 2002.

27. Bittner EA SE, Woodson L, Martyn JA. Acute and perioperative care of the burn-injured patient. *Anesthesiology*. 2015;122(2):448-64.
28. Williams FN, Herndon DN, Jeschke MG. The hypermetabolic response to burn injury and interventions to modify this response. *Clin Plast Surg*. 2009;36(4):583-96.
29. Hart DW WS, Mlcak R, Chinkes DL, Ramzy PI, Obeng MK, Ferrando AA, Wolfe RR, Herndon DN. Persistence of muscle catabolism after severe burn. *Surgery*. 2000;128(2):312-9.
30. Eric Reiss EP, Curtis P. Artz, and Bernard Balikov. The metabolic response to burns. *Journal of Clinical Investigation*. 1956;35(1):62-77.
31. Douglas W. Wilmore M.D. LHAPD, Major, M.S.C. Metabolic Changes in Burned Patients. *Surgical Clinics of North America*. 1978;58(6): 1173-87.
32. Douglas W. Wilmore JML, Arthur D. Mason, Jr., Robert W. Skreen, and Basil A. Pruitt, Jr. Catecholamines: Mediator of the Hypermetabolic Response to Thermal Injury. *Annals of Surgery* 1974;180(4):653–68.
33. DP C. Postshock metabolic response. *Lancet*. 1942;239:433-7.
34. Jeschke MG, Chinkes DL, Finnerty CC, Kulp G, Suman OE, Norbury WB, et al. Pathophysiologic response to severe burn injury. *Ann Surg*. 2008;248(3):387-401.
35. Shehan Hettiaratchy PD. ABC of burns: pathophysiology and types of burns. *BMJ Clinical Review*. 2004;328(7453):1427-9.
36. Tobe E. Progressive neuropsychiatric and brain abnormalities after smoke inhalation. *BMJ Case Rep*. 2012;2012.
37. <Nolte's The Human Brain 6th edition.pdf>.

38. Fuster JM. The prefrontal cortex--an update: time is of the essence. *Neuron*. 2001;30(2):319-33.
39. José L. Lanciego NL, José A. Obeso. Functional Neuroanatomy of the Basal Ganglia. *Cold Spring Harbor Perspectives in Medicine*. 2012;2(12):a009621.
40. M. Ángeles Fernández-Gil RP-B, M. Leo-Barahona, and J.P. Mora-Encinas. Anatomy of the Brainstem: A Gaze Into the Stem of Life. *Seminar in Ultrasound in CT and MRI*. 2010;31(3):196-219.
41. G. Barkhoudarian DFK. The Pituitary Gland: Anatomy, Physiology, and its Function as the Master Gland. In: Edward R. Laws J, editor. *Cushing's Disease: An Often Misdiagnosed and Not So Rare Disorder*: Elsevier Inc; 2017. p. 1-41.
42. Kimura R TL, Herndon DN, Linares HA, Lubbesmeyer HJ, Traber DL. Increasing duration of smoke exposure induces more severe lung injury in sheep. *Journal of Applied Physiology*. 1988;64(3):1107-13.
43. Ihara K FS, Enkhtaivan B, Trujillo R, Perez-Bello D, Nelson C, Randolph A, Alharbi S, Hanif H, Herndon D, Prough D1, Enkhbaatar P. Adipose-derived stem cells attenuate pulmonary microvascular hyperpermeability after smoke inhalation. *PLoS One*. 2017;12(10).
44. Soejima K SF, Sakurai H, Traber LD, Traber DL. Pathophysiological analysis of combined burn and smoke inhalation injuries in sheep. *American Journal of Physiology Lung Cell Molecular Physiology*. 2001;280(6):L1233-41.
45. Bardehle S, Rafalski VA, Akassoglou K. Breaking boundaries-coagulation and fibrinolysis at the neurovascular interface. *Front Cell Neurosci*. 2015;9:354.

46. Cortes-Canteli M, Mattei L, Richards AT, Norris EH, Strickland S. Fibrin deposited in the Alzheimer's disease brain promotes neuronal degeneration. *Neurobiol Aging*. 2015;36(2):608-17.
47. Holly E. Hinson DFH, and Wendy C. Ziai. Management of Intraventricular Hemorrhage. *Current Neurology and Neuroscience Reports*. 2010;10(2):73- 82.
48. Garcia-Rill E. Reticular Activating System. Squire LR, editor. Science Direct Academic Press; 2009. 6 p.
49. Pang D SR, Horton JA. Lysis of intraventricular blood clot with urokinase in a canine model: Part 1. Canine intraventricular blood cast model. *Neurosurgery*. 1986;19(4):540- 6.
50. Steinke W SR, Mohr JP, Foulkes MA, Tatemichi TK, Wolf PA, Price TR, Hier DB. Thalamic stroke. Presentation and prognosis of infarcts and hemorrhages. *Archives of Neurology*. 1992;49(7):703- 10.
51. Hütter BO K-AI, Gilsbach JM. Cognitive deficits in the acute stage after subarachnoid hemorrhage. *Neurosurgery*. 1998;43(5):1054-65.
52. Jaroslaw Aronowski XZ. Molecular Pathophysiology of Cerebral Hemorrhage Secondary Brain Injury. *Stroke*. 2011;42(6):1781-6.
53. Kim DY CY, Jang EW, Chung J, Joo JY, Kim YB. Clinico-radiological Characteristics of Spontaneous Basal Ganglia Hemorrhage, According to Regional Classification. *Journal of Cerebrovascular and Endovascular Neurosurgery*. 2014;16(3):216-24.

54. Su CY CH, Kwan AL, Lin YH, Guo NW. Neuropsychological impairment after hemorrhagic stroke in basal ganglia. *Archives of Clinical Neuropsychology*. 2007;22(4):465–74.
55. Kim DH KS, Cho Y, Jung TM, Ahn SJ, Park YG. Usefulness of voxel-based lesion mapping for predicting motor recovery in subjects with basal ganglia hemorrhage: A preliminary study with 2 case reports. *Medicine*. 2016;95(23):1-5.
56. Furuse M KK, Miyashita M, Saura R, Kuroiwa T. A case of hypertensive intraventricular hemorrhage bled from the hippocampus. *Neurological Sciences*. 2012;33(2):317-9.
57. MR. Q-P. Clinical approach to brainstem lesions. *Semin Ultrasound CT MR*. 2010;31(3):220-9.
58. Tsunoda T MS, Watanabe M, Nagai A, Ueno Y, Ozeki Y, Okamoto S, Mizuno S, Sonoda Rehabilitation for a Patient with Hemiplegia, Ataxia, and Cognitive Dysfunction Caused by Pontine Hemorrhage. *Casre Reports in Neurology*. 2015;7(3):213–20.
59. D'aes T MP. Cognitive and affective disturbances following focal brainstem lesions: a review and report of three cases. *Cerebellum*. 2015;14(3):317-40.
60. Jensen MB SLE. Management of acute cerebellar stroke. *Archives of Neurology*. 2005;62(4):537-44.
61. Ilse Vanhorebeek LL, Greet Van den Berghe. Endocrine aspects of acute and prolonged critical illness. *Nature Clinical Practice Endocrinology and Metabolism*. 2006;2(1):20-31.
62. Saloua Akoudad M, PhD; Frank J. Wolters, MD; Anand Viswanathan, MD, PhD; Renée F. de Bruijn, MD, PhD; Aad van der Lugt, MD, PhD; Albert Hofman, MD, PhD;



Peter J. Koudstaal, MD, PhD; M. Arfan Ikram, MD, PhD; Meike W. Vernooij, MD, PhD.

Association of Cerebral Microbleeds With Cognitive Decline and Dementia. *JAMA*

*Neurology*. 2016;73(8):934-43.

63. Poels MM IM, van der Lugt A, Hofman A, Niessen WJ, Krestin GP, Breteler MM, Vernooij MW. Cerebral microbleeds are associated with worse cognitive function: the Rotterdam Scan Study. *Neurology*. 2012;78(5):326-33.

64. Davalos D AK. Fibrinogen as a key regulator of inflammation in disease. *Seminars in Immunopathology*. 2012;34(1):43-62.

65. Strecker JK SA, Schäbitz WR, Minnerup J. Neutrophil granulocytes in cerebral ischemia – Evolution from killers to key players. *Neurochemistry International* 2017;107(117-126):117.

## Vita

Anita Randolph was born on June 18<sup>th</sup>, 1987 in Atlanta, GA to Patrick Randolph and Tamara Elder. In 2011, she graduated from the University of Georgia with a Bachelors of Science in Genetics and Microbiology and a Bachelors of Agriculture in Animal and Dairy Sciences with an emphasis in Animal Biology.

While at the University of Georgia, she participated in several research organizations. As a research scholar in the Peach State Louis Stokes Alliance for Minority Participation (Peach State LSAMP), Anita Randolph researched in the laboratory of Dr. Steven Stice. The aim of her project was to assess the functionality of glutamate receptors in a neural progenitor cell line derived from WA09 human embryonic stem cells.

After completing her studies at the University of Georgia, she continued to seek opportunities to strengthen her neuroscience knowledge. As a Preparatory Research Experience Postbaccalaureate Program (PREP) Scholar at the University of Alabama at Birmingham, Anita Randolph researched in the laboratory of Dr. Michelle Olsen. Her project focused on alterations in astrocytic protein and gene expression in the pilocarpine model of epilepsy.

In 2014, she started her graduate career at the University of Texas Medical Branch where researched in the Translational Intensive Care Unit (TICU) characterizing central nervous damage after acute exposure to smoke inhalation ± third-degree skin burn injury.

Permanent address:

1733 Valencia Road

Decatur, GA 30032

This dissertation was typed by Anita Randolph